Active galactic nuclei (AGNs): a brief observational tour

Yongquan Xue (薛永泉)

Department of Astronomy
University of Science and Technology of China
http://staff.ustc.edu.cn/~xuey

Summary of lectures

- Early history, AGN ABCs, finding AGNs, AGN terminology and unification
- Dissecting AGNs (I): black hole, accretion disk, broad line region
- Dissecting AGNs (II): torus, narrow line region, stars and starburst regions, jets
- Focused lecture: Lifting the veil of deeply buried supermassive black holes in the Universe

Summary of lectures

- Early history, AGN ABCs, finding AGNs, AGN terminology and unification
- **Dissecting AGNs (I): black hole, accretion disk, broad line region**
- Dissecting AGNs (II): torus, narrow line region, stars and starburst regions, jets
- Focused lecture: Lifting the veil of deeply buried supermassive black holes in the Universe

AGN "Powers of Ten" (Courtesy of Pat Hall)

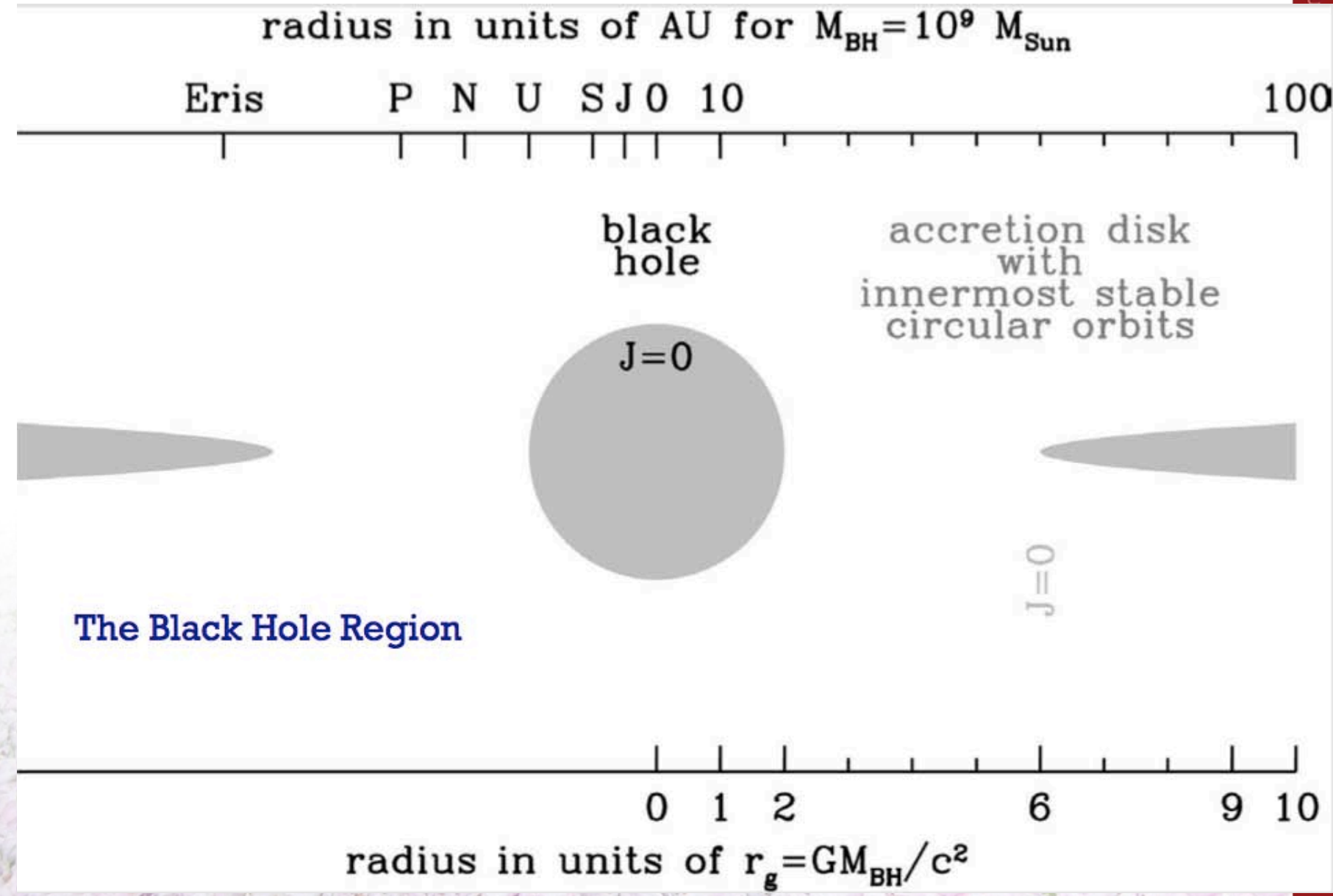

AGN "Powers of Ten" (Courtesy of Pat Hall)

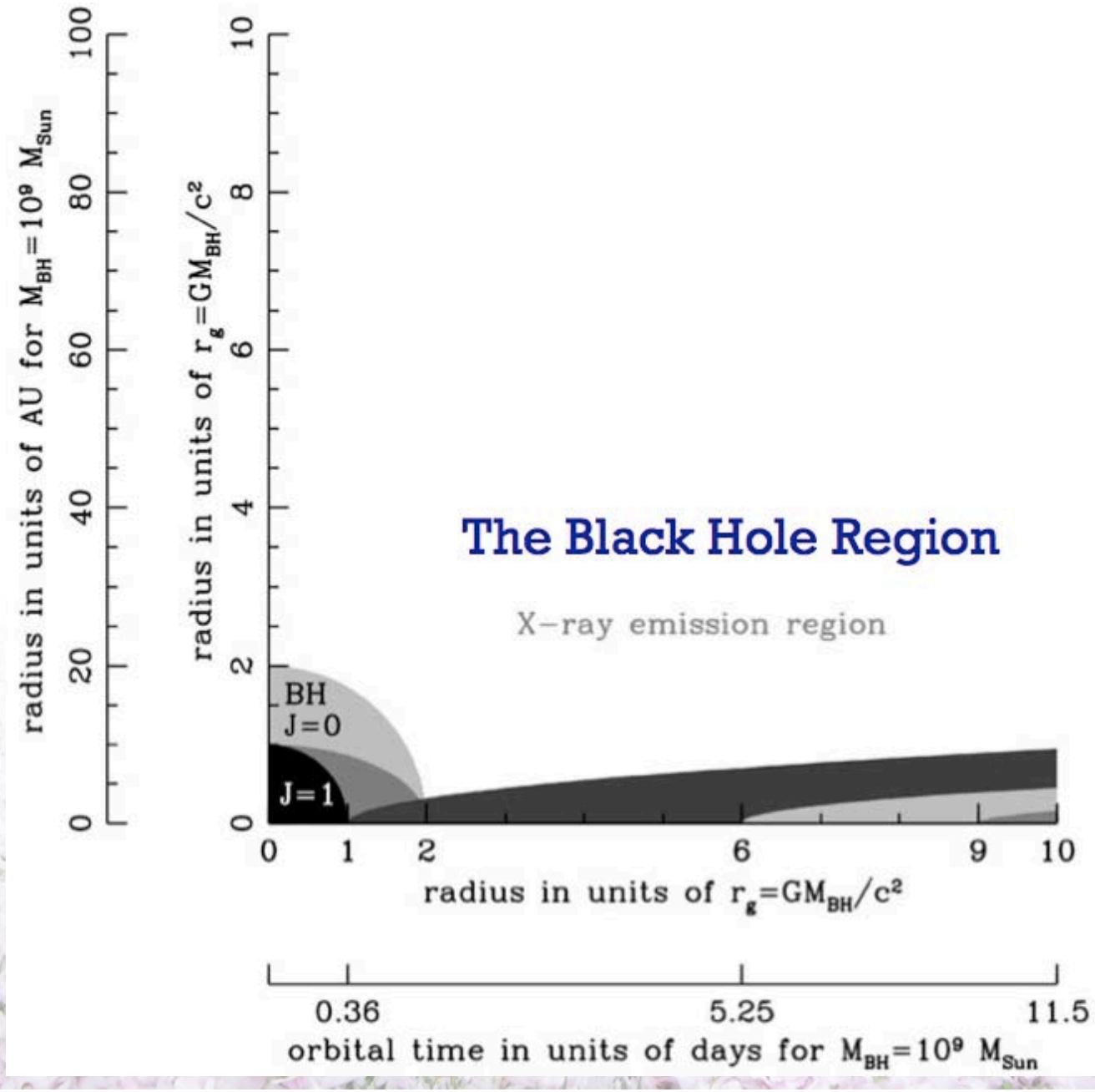

AGN "Powers of Ten" (Courtesy of Pat Hall)

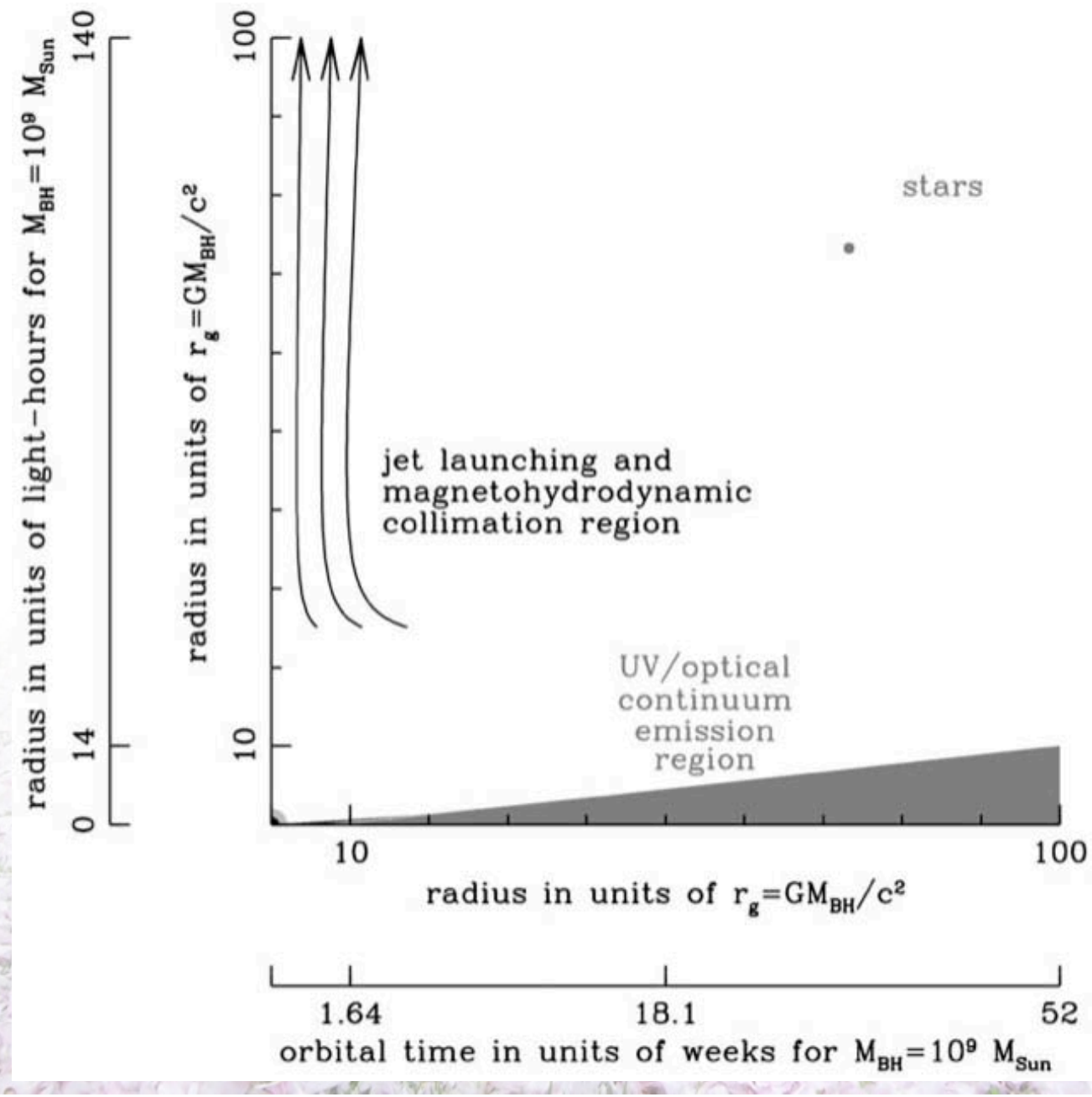

AGN "Powers of Ten" (Courtesy of Pat Hall)

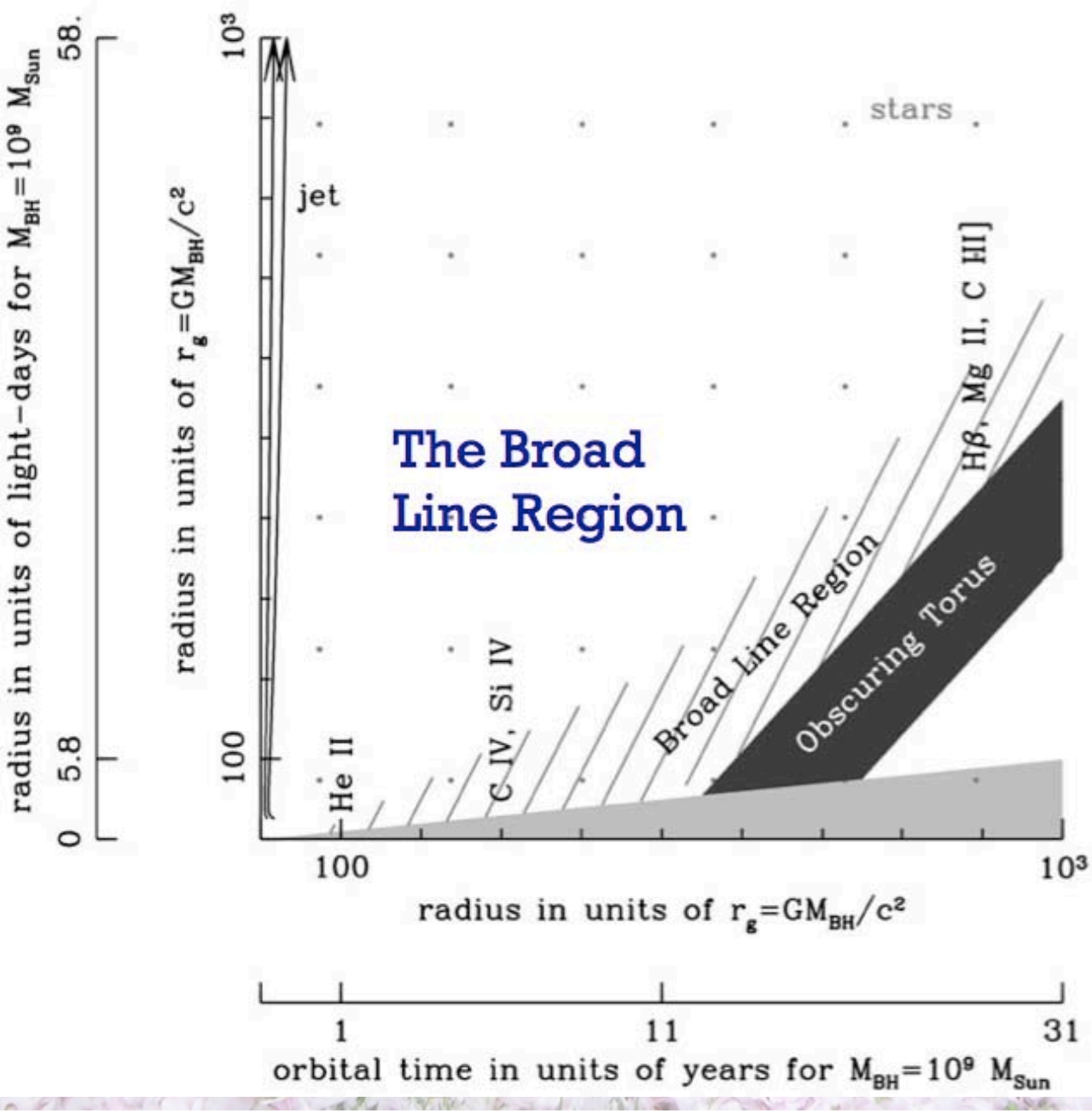

AGN "Powers of Ten" (Courtesy of Pat Hall)

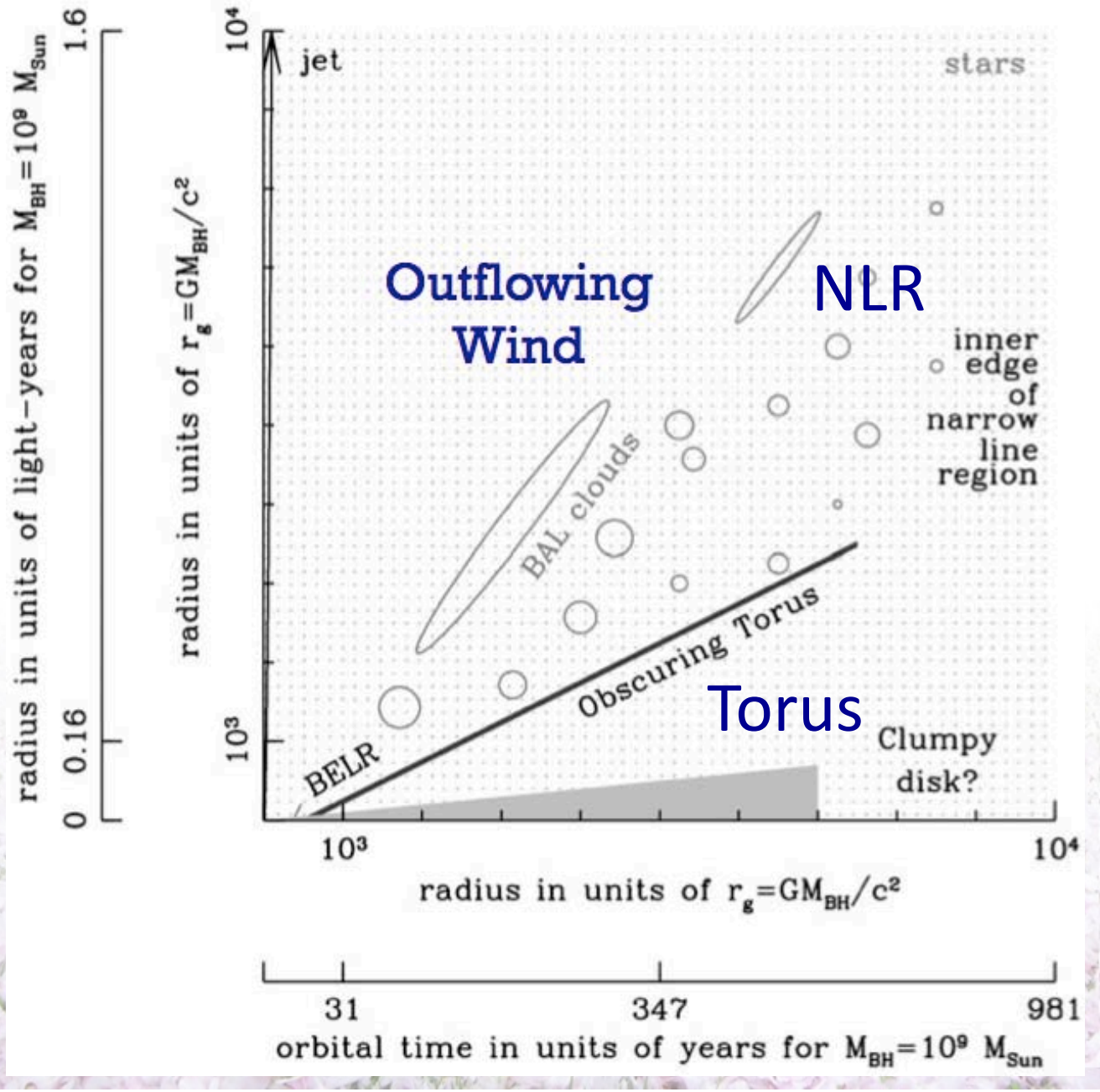

Black hole

Black holes

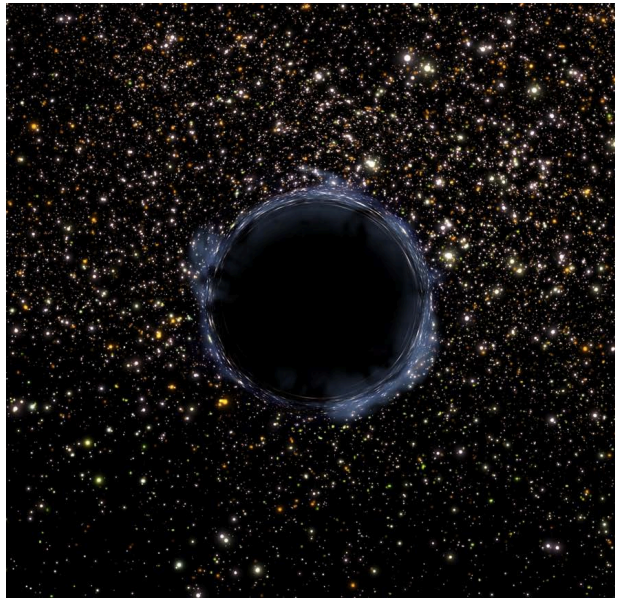

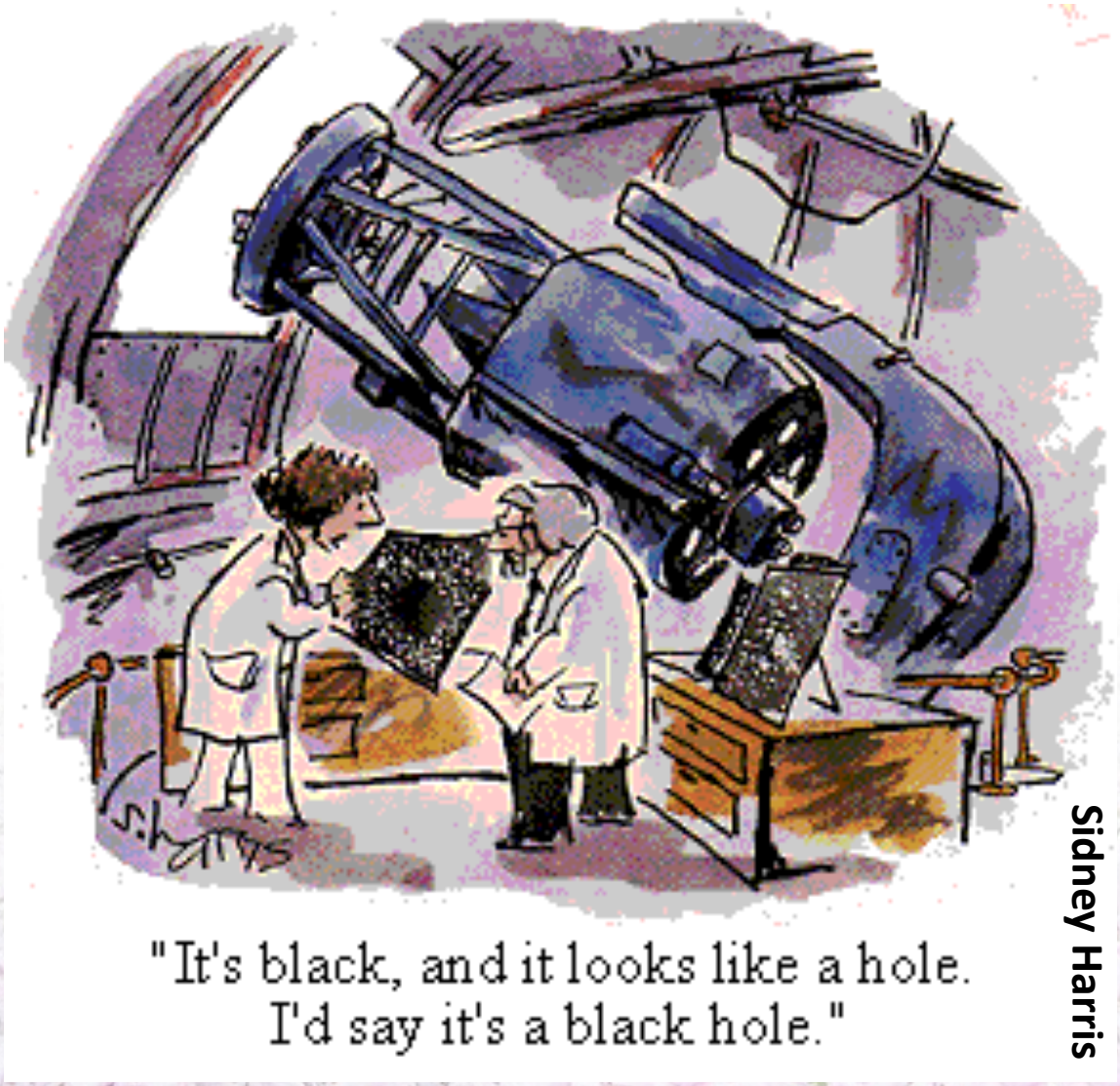

Tidal Disruption Event (TDE): discover quiescent SMBHs

- Not every black hole is “awake”! What about you right now? :)

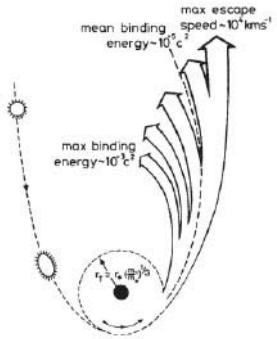

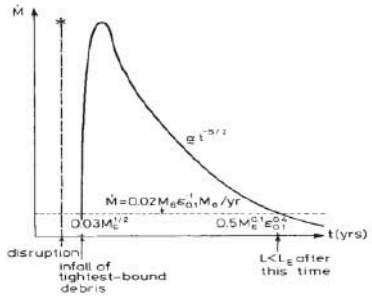

$$R_t = \left(\frac{M_{BH}}{M_*}\right)^{1/3} R_*$$

$$\frac{R_t}{R_s} \approx 23 M_6^{-2/3}$$

rate ~ 10^{-6}~10^{-4} per year

General black hole properties

- BHs: extreme cases of curved space-time; described by GR

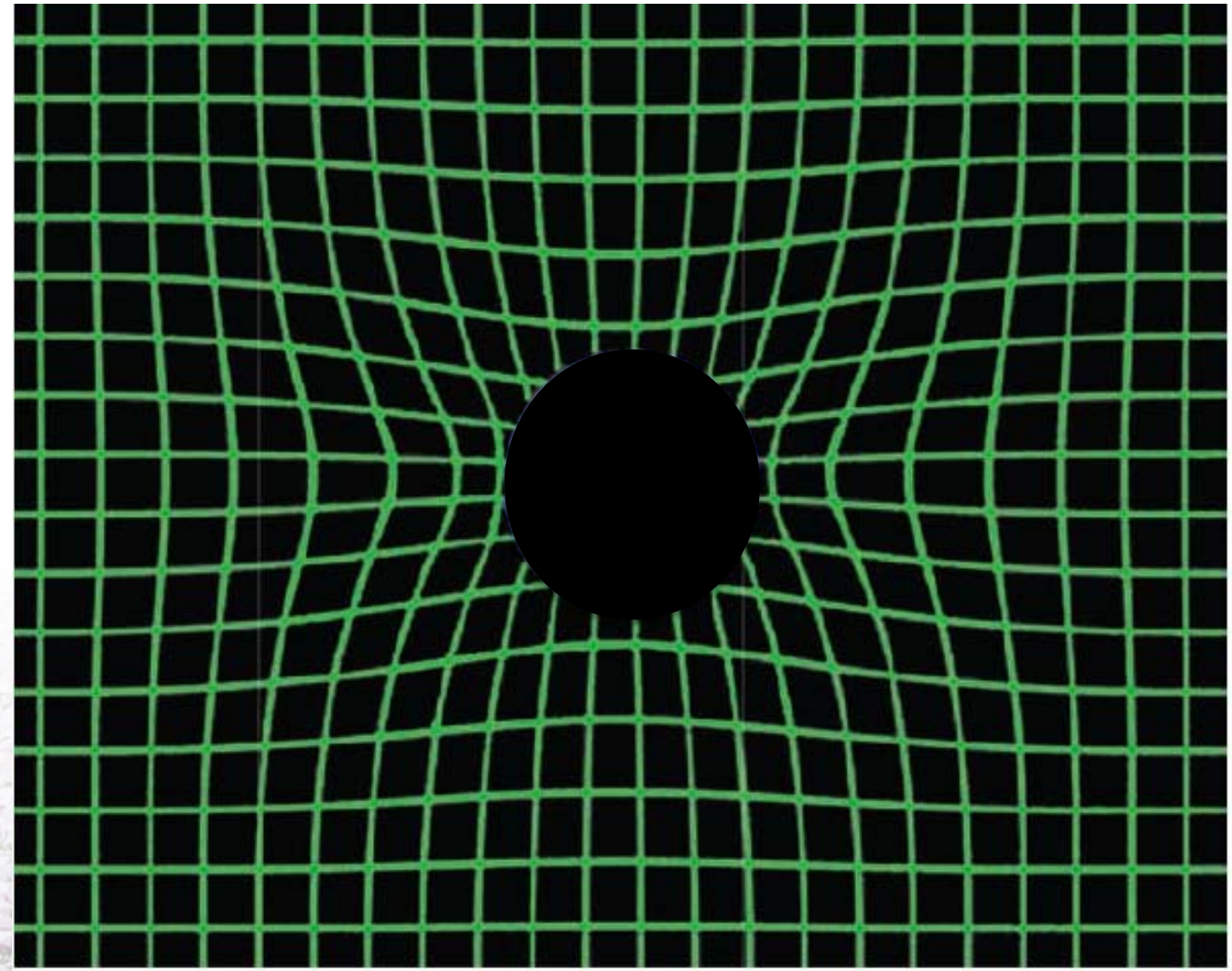

Figure 1.20 A rubber sheet analogy of the distortion of space–time by mass. <<I.A.C.>>

- "no hair" theorem of BHs: can possess only 3 properties – mass, charge, and angular momentum; charge not important in astronomical settings

  - neglect electrically charged BHs and consider only stationary (Schwarzschild) and rotating (Kerr) BHs

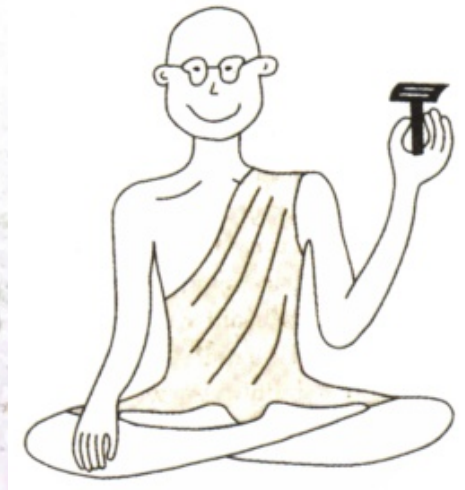

- Gravitational radius $r_g=GM/c^2 \sim 1.5e13\ M_8$ cm (M_8: BH mass in units of 1e8 Msun; cf. 1pc=3e18 cm)
- All properties of stationary BHs can be described by using r_g
- For rotating/spinning BHs, introduce additional quantities:

  - angular momentum s (J more frequently used)

$$s \sim I\Omega \simeq Mr_g^2\left(\frac{v}{r}\right) \simeq Mr_g c$$

  - specific angular momentum (i.e., angular momentum per unit mass)

$$s/M \equiv \alpha c$$

  where alpha is the specific angular diameter

  - dimensionless spin parameter: $a=sc/GM^2$ ($-1<=a<=1$; +/- rotation direction)

  * $\alpha = ar_g$ or $s/M = ar_g c$
  * when a=1, specific angular momentum $s/M = r_g c \sim 5\times 10^{23} M_8\ \mathrm{cm^2\ s^{-1}}$

  - spin determines max energy that can be extracted from BH during accretion

  * in thin accretion disk: difference of a=0-1 translates to a factor of ~10 in radiation conversion efficiency

- The exact GR expression for the line element ds^2 and its varous solutions that depend on a:

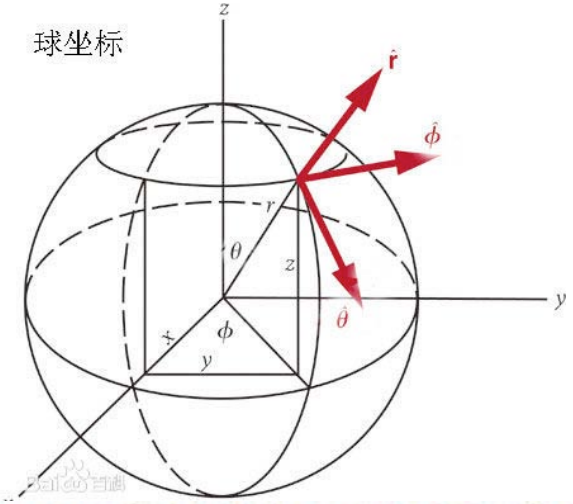

The GR line element near a rotating BH was first derived by Kerr in 1963 (hence the name *Kerr BH*). It is given by

$$ds^2 = \left(1 - \frac{2r_g r}{\Sigma}\right) c^2 dt^2 + \frac{4\alpha r_g r \sin^2\theta}{\Sigma} dt d\phi - \frac{\Sigma}{\Delta} dr^2$$

$$- \Sigma d\theta^2 - \left(r^2 + \alpha^2 + \frac{2r_g r \alpha^2 \sin^2\theta}{\Sigma}\right) \sin^2\theta d\phi^2, \qquad (3.6)$$

where

$$\Sigma = r^2 + \alpha^2 \cos^2\theta \qquad (3.7)$$

$$\Delta = r^2 - 2r_g r + \alpha^2. \qquad (3.8)$$

This expression can be solved for the location of the event horizon of the hole. The

- Simplest solution: a stationary BH with a=0 and alpha=0
  - event horizon (EH) is given by Schwarzschild radius $r_s=2r_g$
- When a!=0, two solutions for EH: $r_\pm = r_g\left[1 \pm (1-a^2)^{1/2}\right]$
  - if a=1, the outer radius is $r_+=r_g$
  - if a=0, the outer radius is $r_+=2r_g=r_s$
  - besides two EHs, Kerr metric also features an additional surface of interest called the static limit, given by $r_0 = r_g\left[1+(1-a^2\cos^2\theta)^{1/2}\right]$
    * the region of space between r_0 and r_+ is called the ergosphere

- Innermost stable circular orbit (ISCO):
  - GR enables us to calculate the orbits of particles in the vicinity of stationary and rotating BHs, in particular, the location of ISCO, i.e., the marginal stability radius, r_{ms} (r_{ISCO} more frequently used)
    * within r_{ms}, particles lose orbital motion and fall directly into EH
    * For Schwarzschild BHs, $r_{ms}=6r_g$
    * For rotating Kerr BHs with a>0, $r_g<=r_{ms}<=6r_g$, exact value depends on a

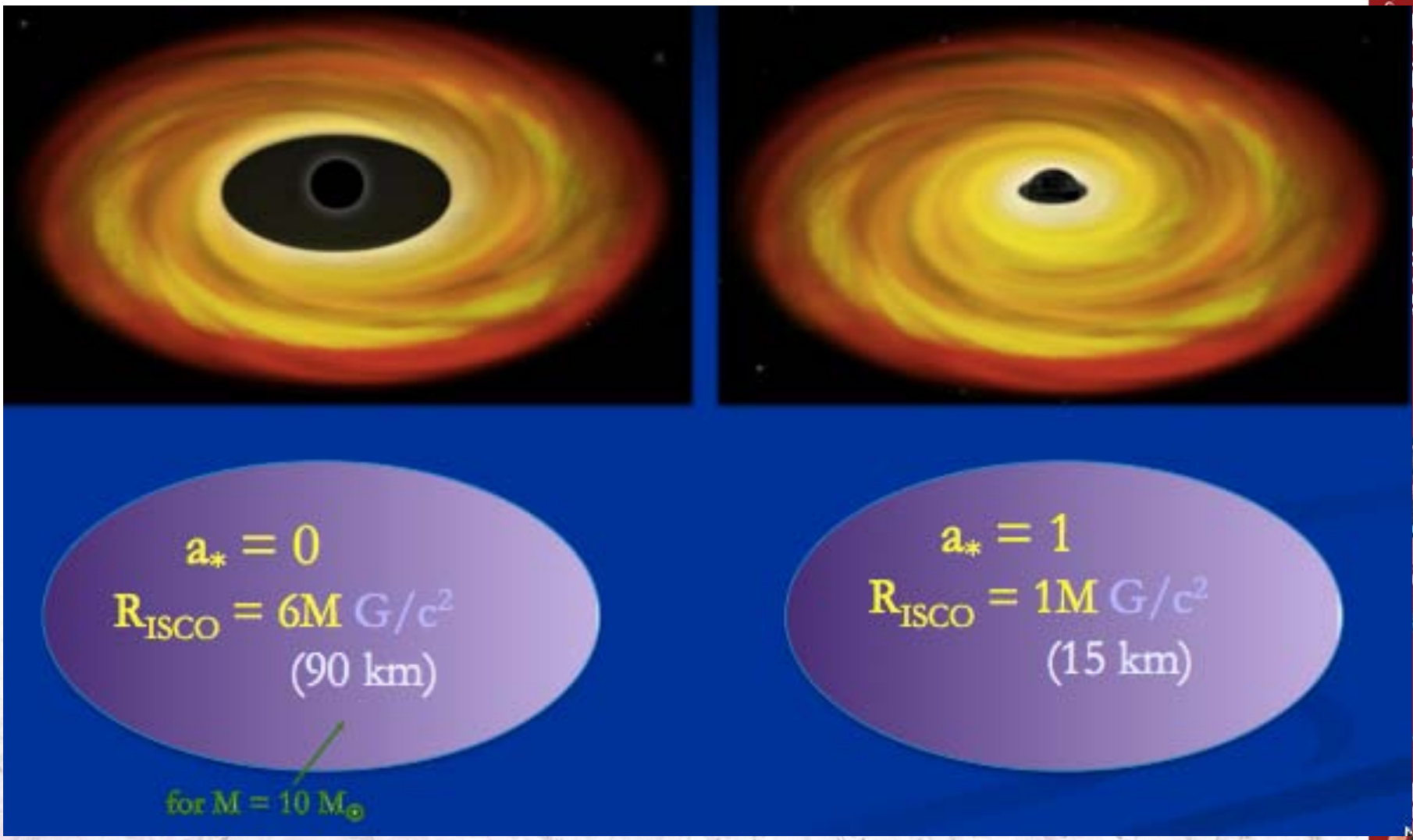
$a_* = 0$
$R_{ISCO} = 6M\ G/c^2$
(90 km)
for M = 10 $M_\odot$
$a_* = 1$
$R_{ISCO} = 1M\ G/c^2$
(15 km)

Iron Kα Line

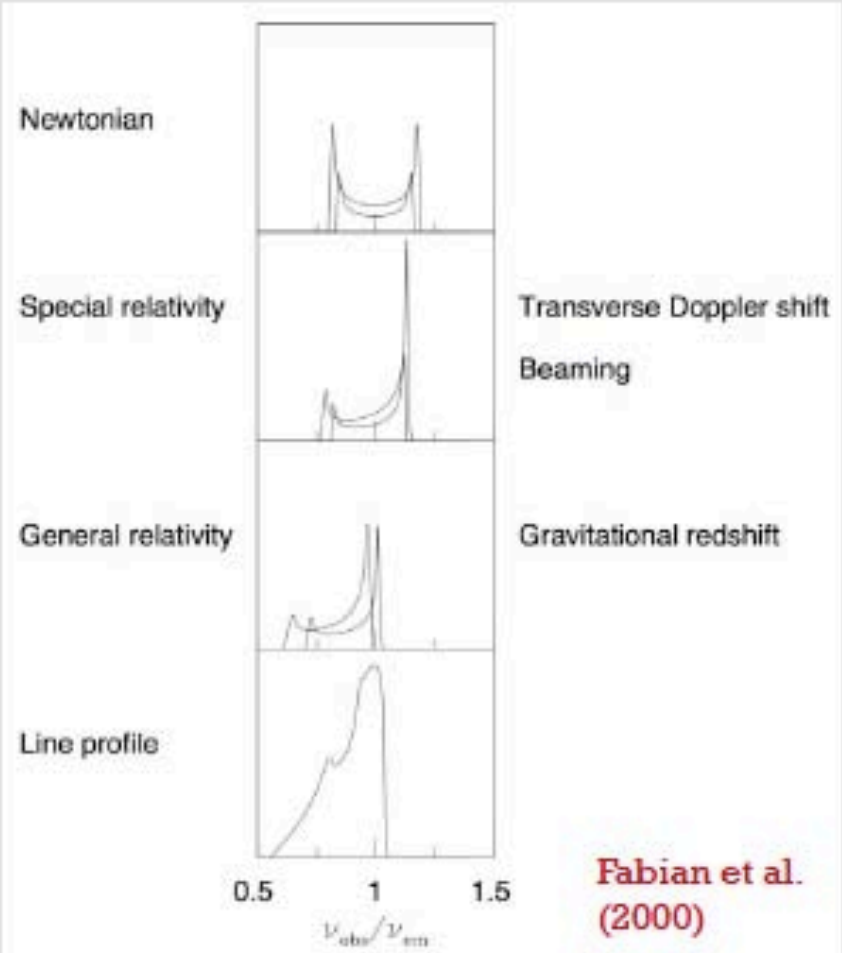

Fabian et al. (2000)

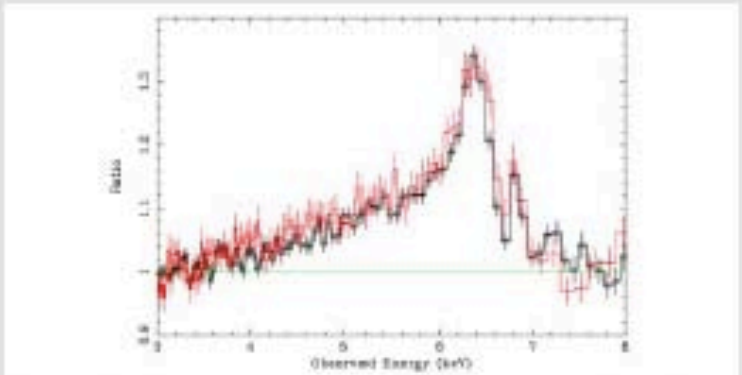

Figure 4: The figure above shows the relativistic disk line profile revealed in MCG-6-30-15 after fitting for the continuum. (Adapted from Miniutti et al. 2007 and Reeves et al. 2006.) The line in MCG-6-30-15 is the best example known presently, and these spectra above are the best yet obtained. The spectrum in black was obtained with *Suzaku*, and the spectrum in red was obtained with *XMM-Newton*.

Made via iron fluorescence when disk irradiated by X-rays.

Iron has best product of abundance and fluorescent yield.

With very high-S/N data, can use to estimate disk inclination, disk emissivity, and black-hole spin.

- If we use the notation x=r/r_g, GR calculations show $\eta = 1 - \left[1 - \frac{2}{3x}\right]^{1/2}$
  - for Schwarzschild BHs, x=6, η=0.057 (Newtonian approx. gives 1/12)
  - overall range in the efficiency of accretion processes: η ~0.038-0.421
  - BH accretion: very efficient!

Table 3.1. *Properties of Schwarzschild and Kerr BHs*

a	r_{ms}/r_g	η
−1.0	9.0	0.038
0	6.0	0.057
0.1	5.67	0.061
0.5	4.23	0.082
0.9	2.32	0.156
0.998	1.24	0.321
1.0	1.00	0.423

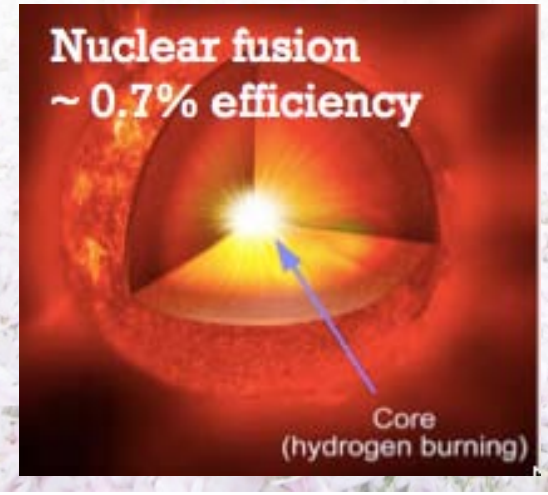

- Specific angular momentum of BH vs. that on typical galactic scales:
  - galactic scales: if r=1 kpc, rotational velcocity v=300 km s^{-1}, then $rv \sim 10^{29}\ \mathrm{cm^2\ s^{-1}}$, which is many orders of mag. larger than $r_g c$
  - if this gas is to be brought to BH vicinity, there must be an efficient mechanism to get rid of excess angular momentum and enable its inflow into the center on timescales typical of galactic evolution
    * on very large physical scales and long timescales, galaxy collision and mergers, bar instability, and other internal (secular) processes are capable of bringing faraway gas into 1-100 pc from the BH
    * still unknown mechanisms: overcome the “100 or 10 pc barrier” and bring the gas to 1e5 r_g or even closer to the BH (last pc problem)

SMBH growth

- Journey of mass accretion

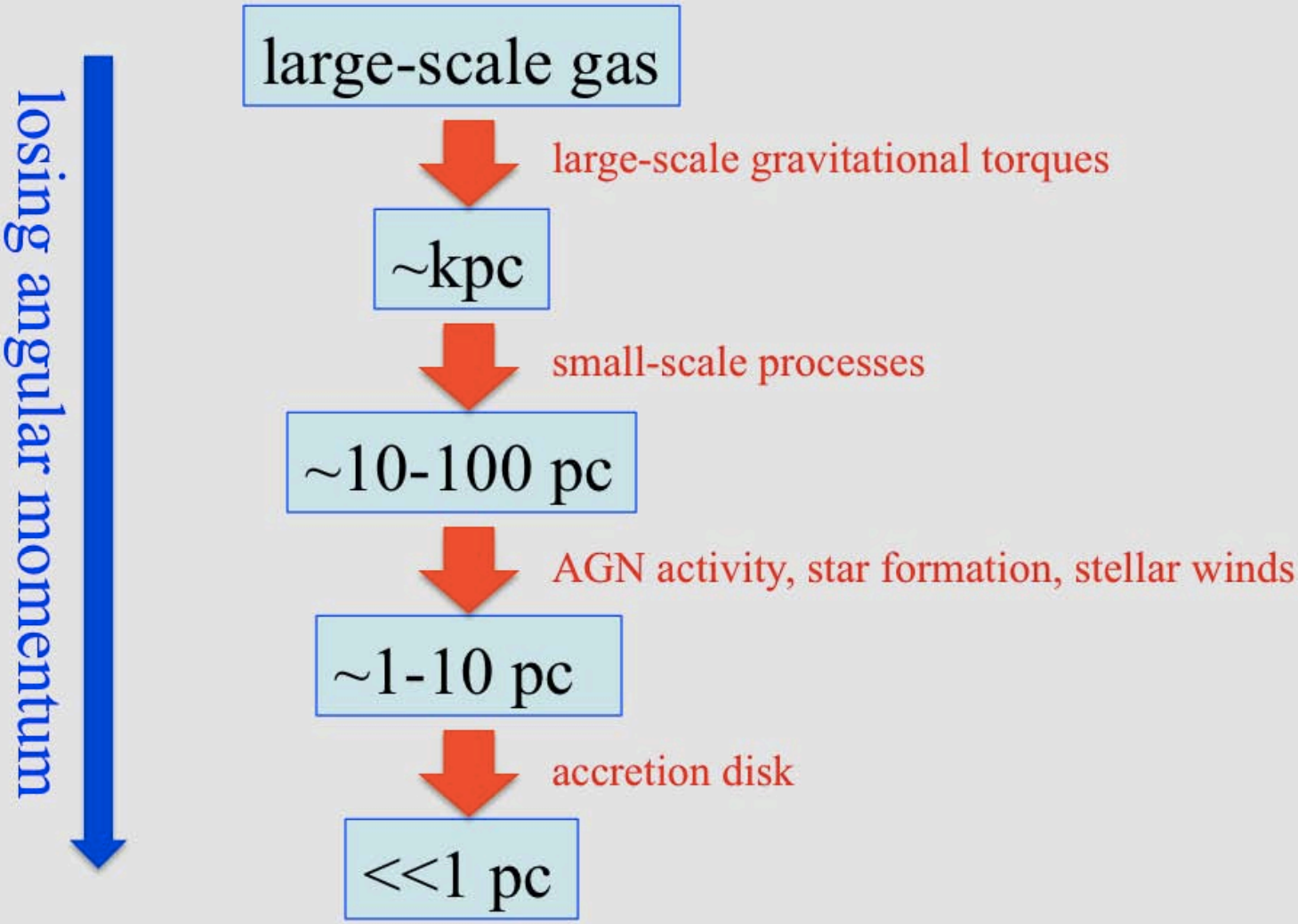

Accretion onto black holes

- Cannot image the main emission regions
  - observed variability implies main emission regions having sizes of light hours to light days (or less)
  - even for close AGNs, this implies angular size of ~1e-6 to 1e-5 arcsec, too small to image directly (cf. VLBA interferometry ~0.0002 arcsec)
  - artist's impressions below



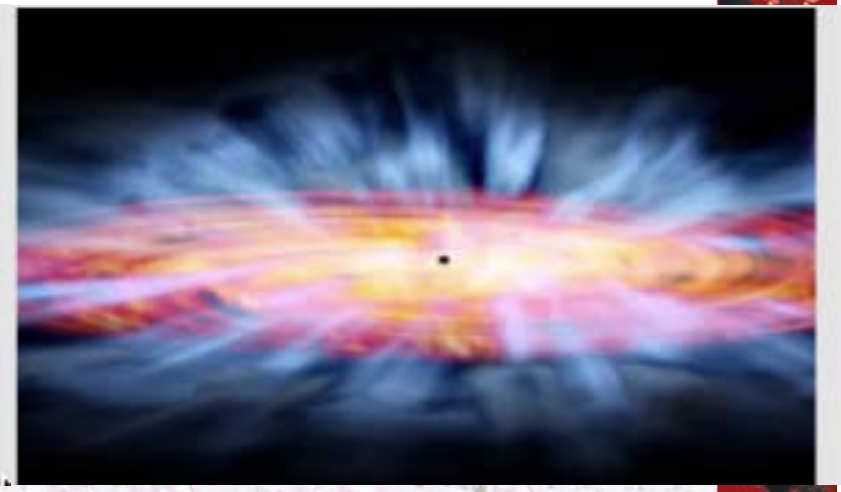

Accretion disk

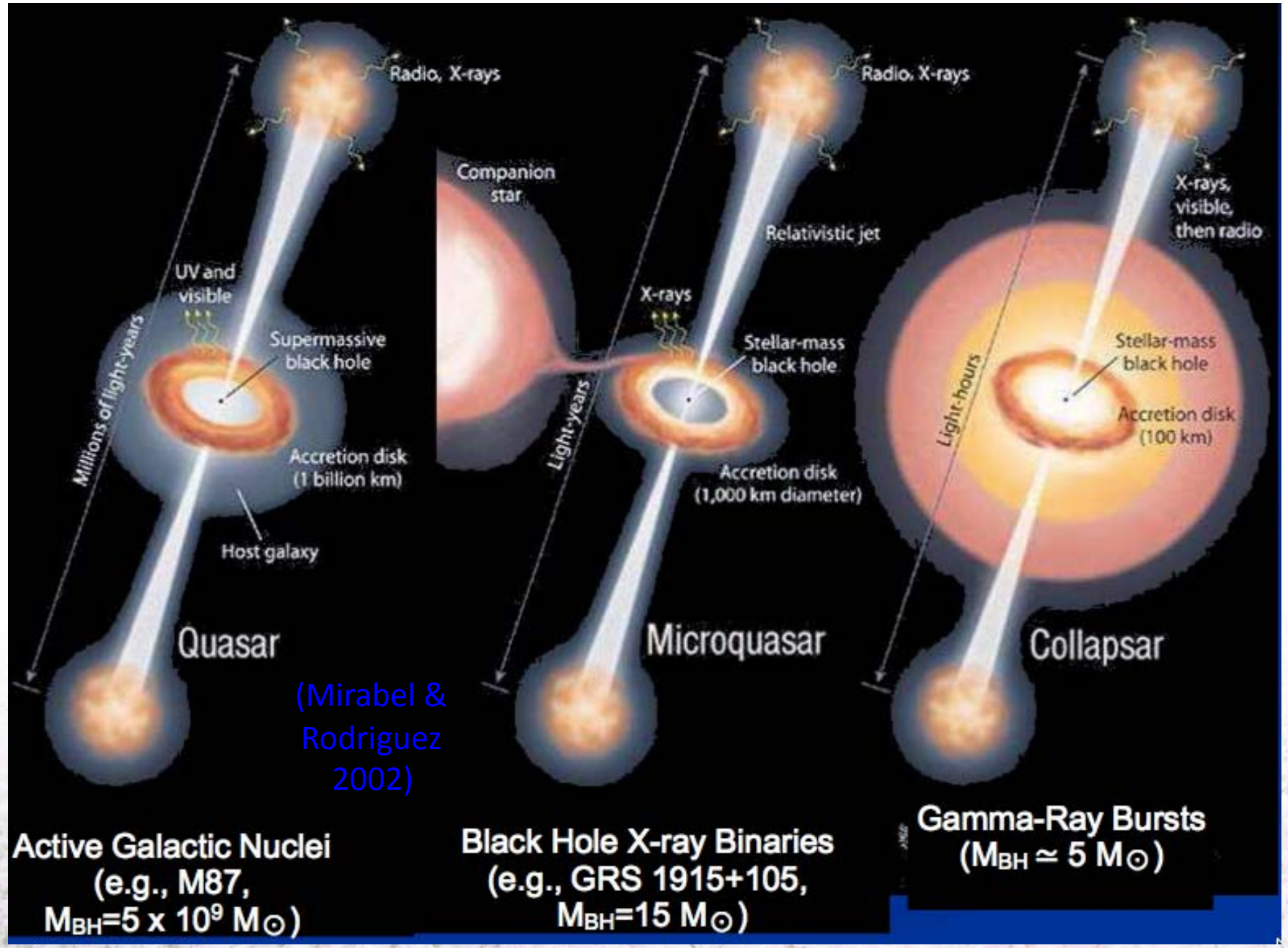

(Mirabel & Rodriguez 2002)

- Common key ingredients: BH, AD, jets

- ADs: hydrodynamics (HD)

  - continuity equation:

$$\frac{\partial \rho}{\partial t} + \nabla \cdot (\rho \boldsymbol{v}) = 0$$

mass conservation

  - momentum equation:

$$\rho \frac{d\boldsymbol{v}}{dt} = -\nabla P - \rho \nabla \Phi$$

mom. conservation

  where the Lagrangian derivative:

$$\frac{d}{dt} \equiv \frac{\partial}{\partial t} + \boldsymbol{v} \cdot \nabla$$

going with the flow element

  - energy equation:

$$\rho \frac{\mathrm{d}(e/\rho)}{\mathrm{d}t} = -P \nabla \cdot \boldsymbol{v}$$

energy conservation

  - equation of state:

$$P = \frac{\rho}{\mu m_p} kT$$

  - boundary conditions: differential --> algebra equations

- ADs: magnetohydrodynamics (MHD)
  - HD + Lorentz force (← Maxwell equations)
  - need one additional equation to evolve the magnetic field
    * Faraday's law (induction equation): $\frac{\partial \boldsymbol{B}}{\partial t} = -c\nabla \times \boldsymbol{E}$
  - assume ideal MHD: gas is a perfect electric conductor
    * the induction equation can be written as: $\frac{\partial \boldsymbol{B}}{\partial t} = \nabla \times (\boldsymbol{v} \times \boldsymbol{B})$

Strong field: matter move along field lines (beads on a wire).

Weak field: field lines are forced to move with the gas.

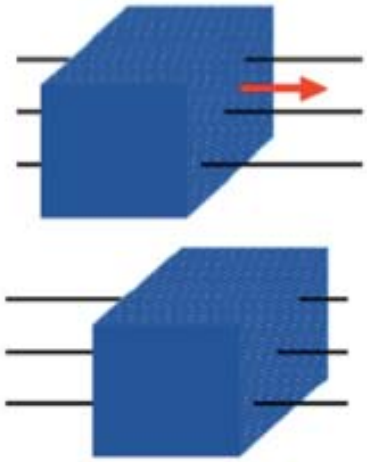

Ideal MHD

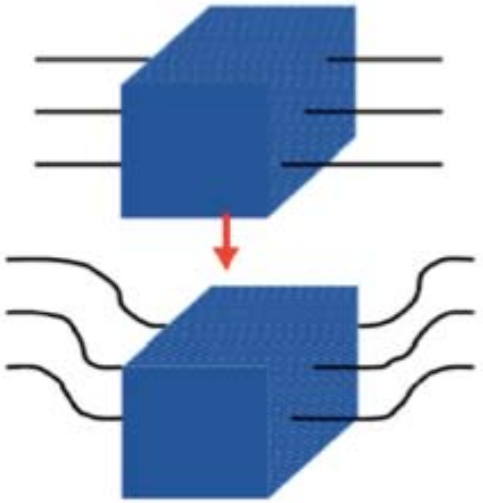

$\frac{|B|^2}{8\pi} >> P_{gas} + \rho|\mathbf{v}|^2$

$\frac{|B|^2}{8\pi} << P_{gas} + \rho|\mathbf{v}|^2$

- ADs: viscosity

  - viscous flow (Navier-Stokes viscosity – NS viscosity)

    * Euler's equation and viscous stress tensor:

$$\frac{\partial(\rho \boldsymbol{v})}{\partial t} + \nabla \cdot (\rho \boldsymbol{v}\boldsymbol{v} + P\mathsf{I}) = \nabla \cdot \boldsymbol{\sigma} \qquad \sigma_{ij} = \rho\nu\left(\frac{\partial v_i}{\partial x_j} + \frac{\partial v_j}{\partial x_i} - \frac{2}{3}\delta_{ij}\nabla \cdot \boldsymbol{v}\right)$$

  - physical interpretation: diffusion of momentum – momentum exchange across velocity gradient

  - NS viscosity too small, so we need an 'anomalous' alpha-viscosity

    * MHD simulations give diverse results on alpha

    * alpha increases with the net magnetic flux, ranging from ~0.01-1

  - disk properties that can affect viscosity:

    * local microphysics (e.g., specific atomic or molecular processes)

    * local or global turbulence

    * magnetic field strength and structure

  - results show that the higher the viscosity, the larger is the radial velocity of the inflowing gas; and the inward velocity is much less than the sound speed (i.e., the radial inflow is subsonic)

- ADs: magnetorotational instability (MRI)
  - Rayleigh criteria for unmagnetized rotating disks:
    * unstable if $\frac{d(\Omega R^2)}{dR} < 0$, which is experimentally confirmed
    * all astrophysical disks should be stable based on this criteria
  - include a vertical, well-coupled magnetic field and change the criteria qualitatively:
    * unstable if $\frac{d\Omega}{dR} < 0$
    * all astrophysical disks should be unstable! – MRI (B: not too strong/weak)
  - resulted MHD turbulence: responsible for transport of angular momentum
  - MRI can amplify magnetic field

- ADs: very complicated to find the exact solutions
  - involve HD, MHD, viscosity, and MRI
    * resort to numerical simulations, still extremely challenging
  - consider some simplified cases
    * e.g., no magnetic field

- Classification of AGN disks and ADs in general:
  - based on shape: thin, slim, and thick disks (depend on mass accretion rate)
    * whether being optically thin or thick, depending on column density (or surface density) and level of ionization of the gas
    * optical depth of AGN disks during fast accretion is very large
- Optically thick, geometrically thin ADs:
  - receive most attention
  - easier to treat analytically and numerically
  - a full solution can be used to calculate the emergent disk spectrum and to compare it with observations

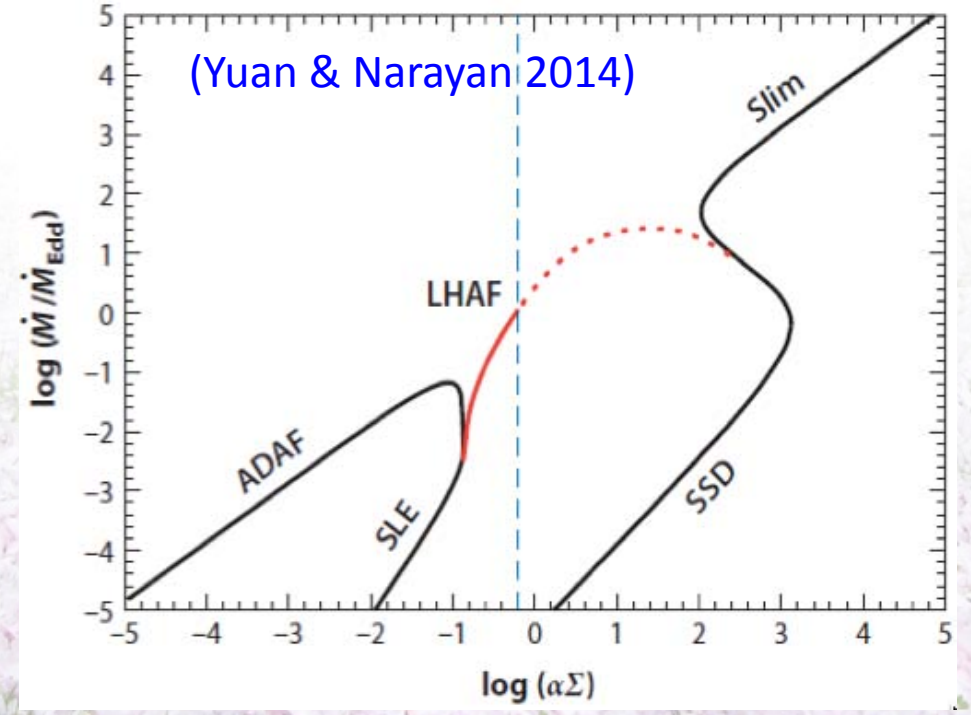

- hot vs. cool
- optically thin vs. thick
- high vs. low accretion rate

Overview of the thin disk model

- Cool: ~10^6 K → Geometrically thin & Keplerian rotation
- Slow radial velocity
- "Optically thick":
- Spectrum: black body spectrum
- Radiative efficiency is high, ~0.1

$$\frac{H_0}{r} = \frac{v_s}{v_K}, \quad v_s \ll v_K$$

A thin disk

Shakura-Sunyaev solution

Under assumptions of:

1) gas pressure dominated;
2) \alpha-viscosity; $\nu = \alpha' v_s H$, $\alpha = \frac{3\alpha'}{2}$
3) Roseland opacity well approximated by Kramer's law

$$
\begin{aligned}
\Sigma &= 5.2\alpha^{-4/5}\dot{M}_{16}^{7/10} m_1^{1/4} R_{10}^{-3/4} f^{14/5}\ \mathrm{g\ cm^{-2}}, \\
H &= 1.7\times10^{8}\alpha^{-1/10}\dot{M}_{16}^{3/20} m_1^{-3/8} R_{10}^{9/8} f^{3/5}\ \mathrm{cm}, \\
\rho &= 3.1\times10^{-8}\alpha^{-7/10}\dot{M}_{16}^{11/20} m_1^{5/8} R_{10}^{-15/8} f^{11/5}\ \mathrm{g\ cm^{-3}}, \\
T_c &= 1.4\times10^{4}\alpha^{-1/5}\dot{M}_{16}^{3/10} m_1^{1/4} R_{10}^{-3/4} f^{6/5}\ \mathrm{K}, \\
\tau &= 190\alpha^{-4/5}\dot{M}_{16}^{1/5} f^{4/5}, \\
\nu &= 1.8\times10^{14}\alpha^{4/5}\dot{M}_{16}^{3/10} m_1^{-1/4} R_{10}^{3/4} f^{6/5}\ \mathrm{cm^2\ s^{-1}}, \\
v_R &= 2.7\times10^{4}\alpha^{4/5}\dot{M}_{16}^{3/10} m_1^{-1/4} R_{10}^{-1/4} f^{-14/5}\ \mathrm{cm\ s^{-1}}, \\
\text{with } f &= \left[1-\left(\frac{R_*}{R}\right)^{1/2}\right]^{1/4}.
\end{aligned}
$$

$$T\left(\frac{r}{r_g}\right) \propto M_8^{-1/4}\left[\frac{\dot{M}}{\dot{M}_{\rm Edd}}\right]^{1/4}\left[\frac{r}{r_g}\right]^{-3/4} f(r)$$

$$f(r) = 1-\left(\frac{r_{\rm in}}{r}\right)^{1/2}$$

- Such disks emit most of E in UV for AGNs, while X-rays for stellar BHs: ~$M^{-1/4}$
- Multi-temperature blackbody emission: temperature~radius$^{-3/4}$

Emitted spectrum of a standard thin disk

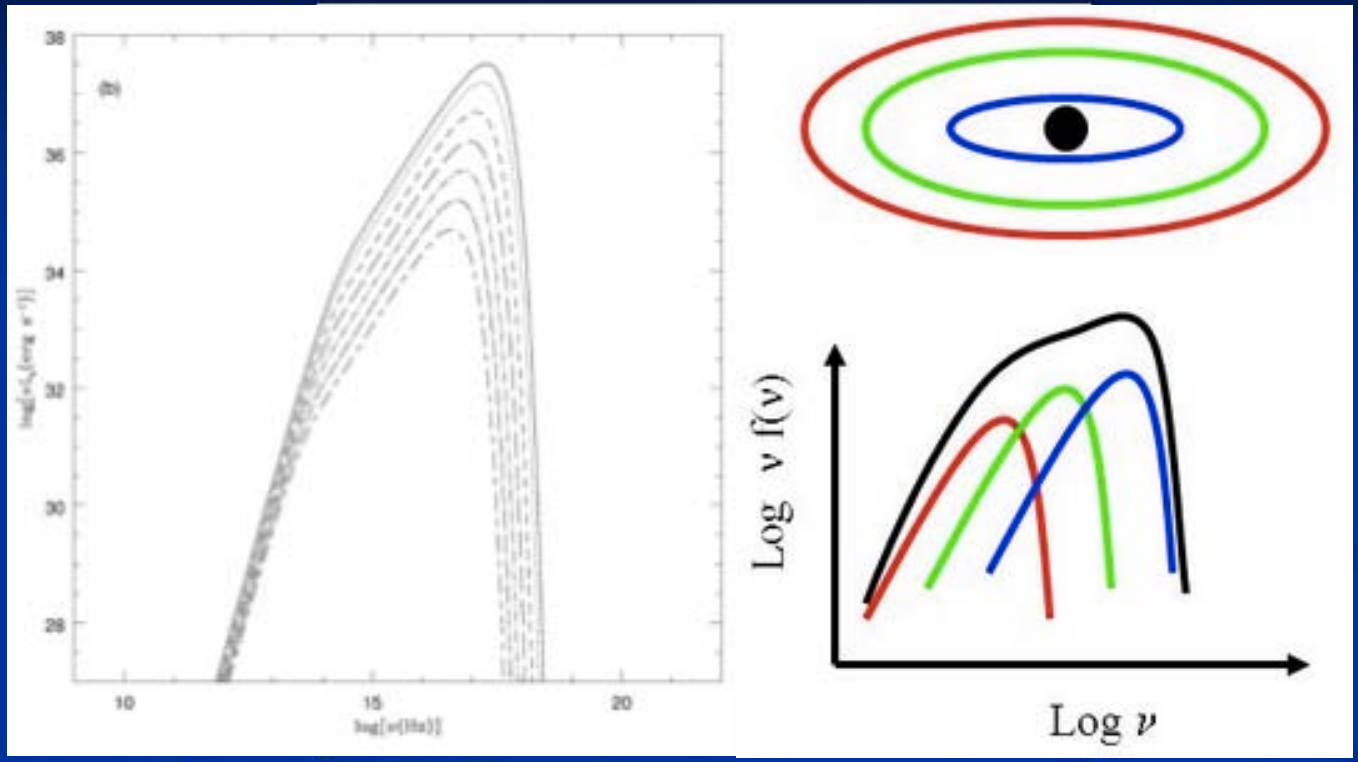

Note that within a radius, the main opacity mechanism is no longer Kramers' opacity, but electron scattering. Since it is no longer involves the microscopic inverse of the processes emitting the radiation (free-free and bound-free) the emergent radiation need not be precisely blackbody, even for quite large optical depth.

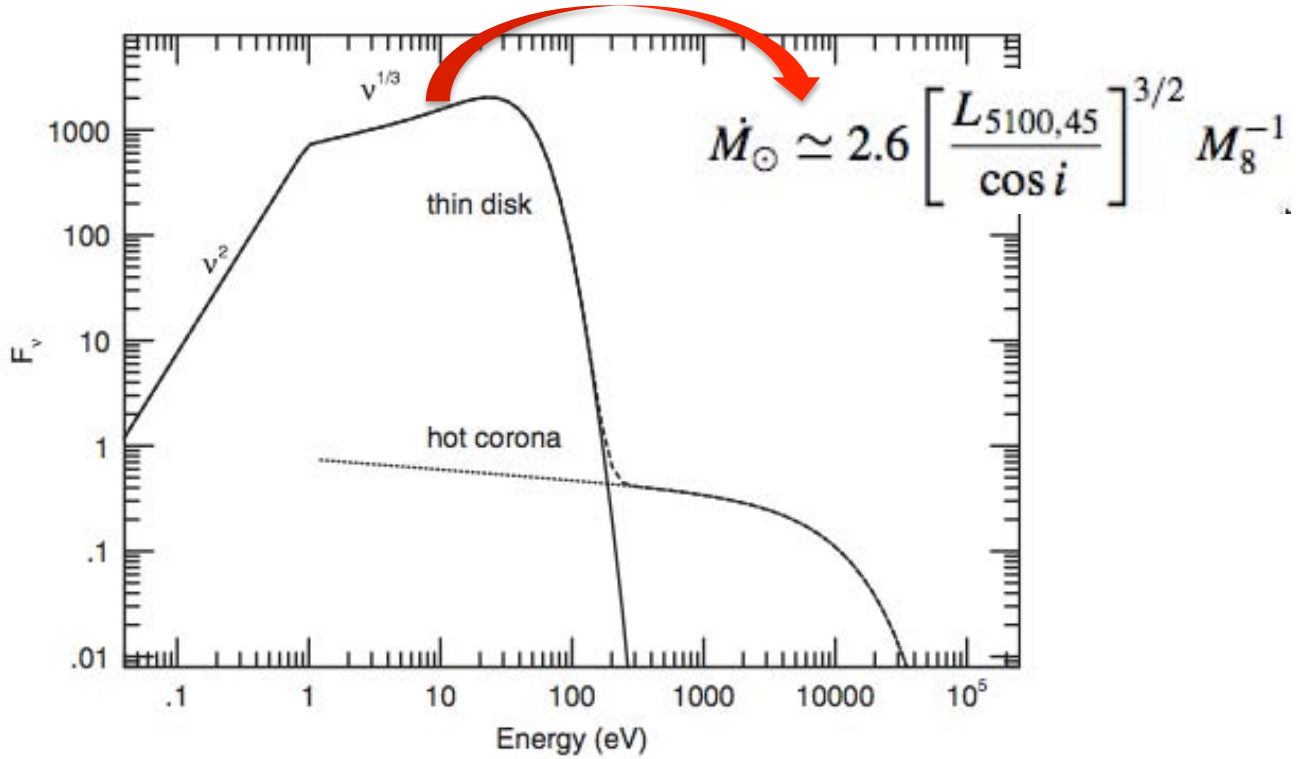

Figure 4.3. A schematic of a combined disk–corona spectrum. The maximum temperature of the geometrically thin, optically thick accretion disk is $T_{\max} = 10^5$ K, and its outer boundary temperature is determined by the conditions at the self-gravity radius. The disk is surrounded by an optically thin corona with $T_{\rm cor} = 10^8$ K.

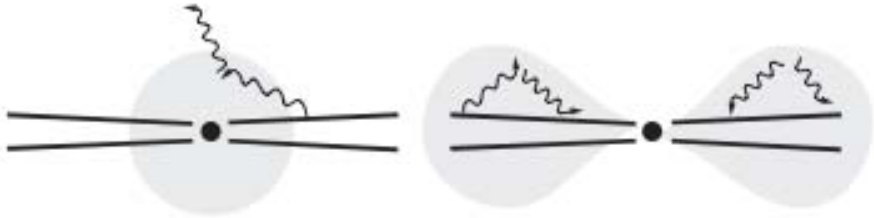

Figure 4.6. Two schematic disk–corona structures showing possible locations of the corona and the scattering geometry of the disk-produced and corona-produced photons.

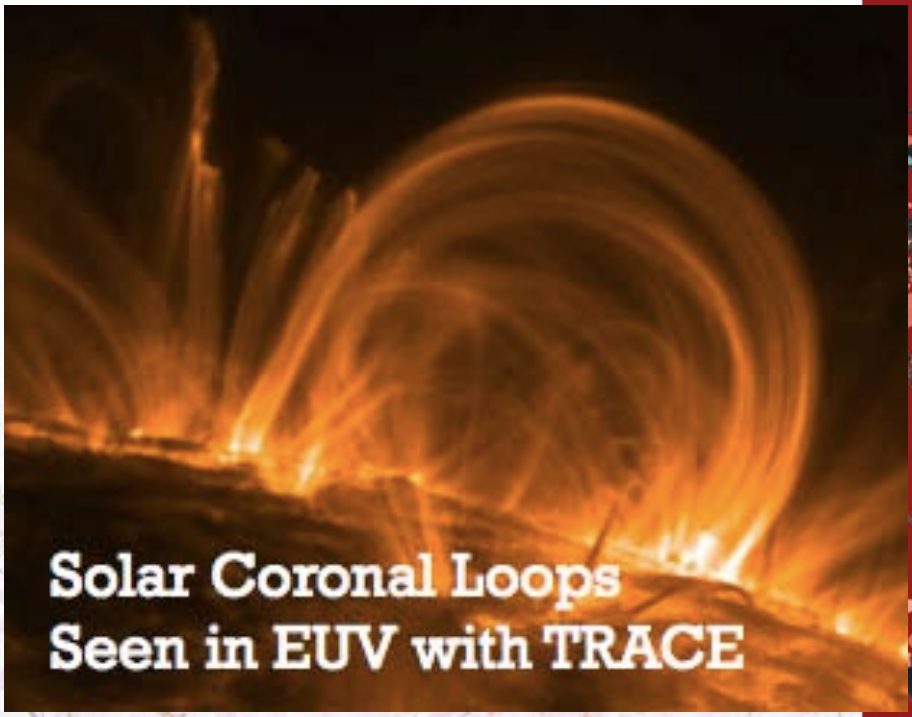

X-ray Emission from Active Galactic Nuclei

Nearly universal from luminous AGNs. From immediate vicinity of black hole.

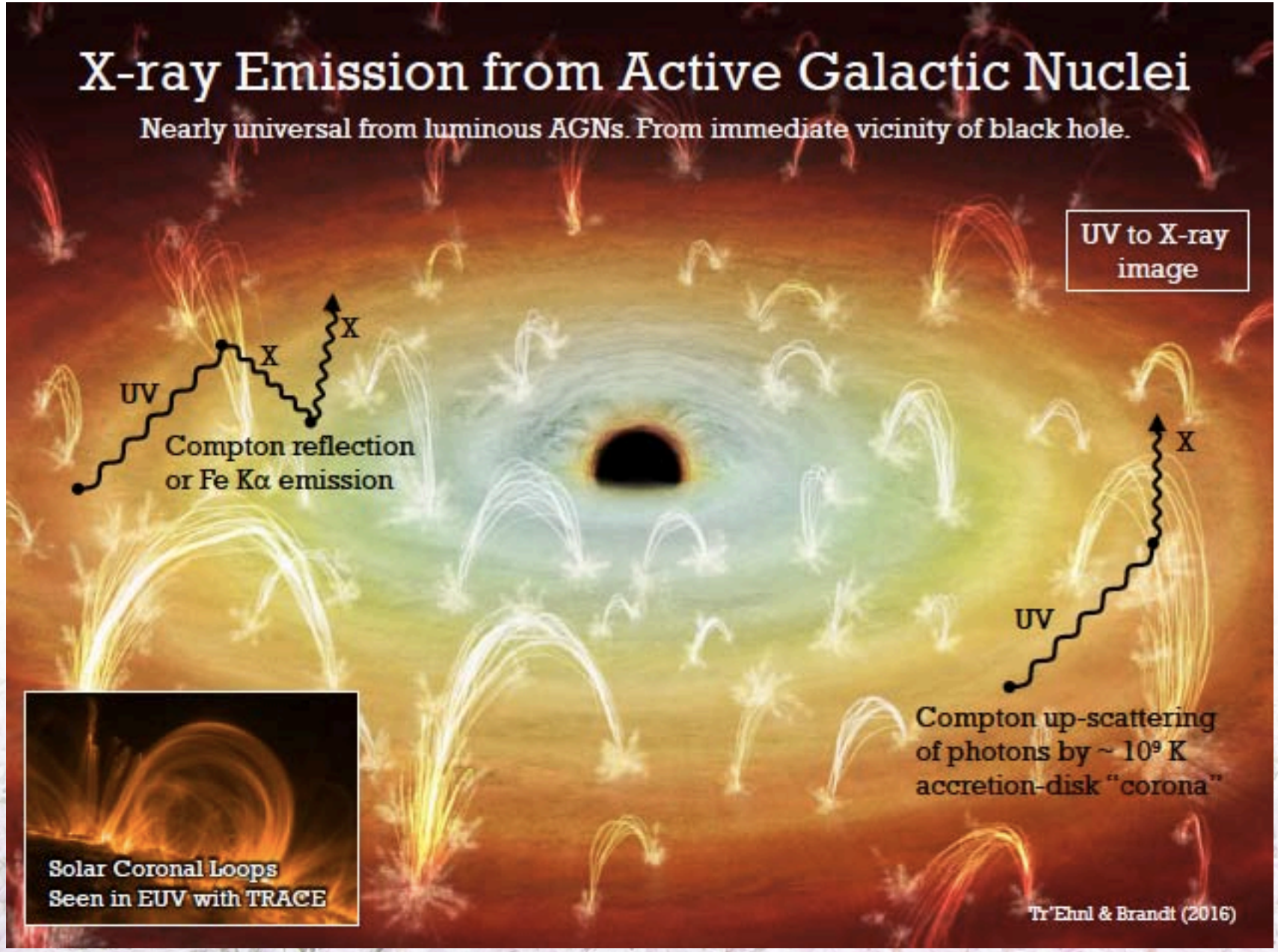

Disc-corona model

- Motivation
  - To explain X-ray radiation
  - Analogy with solar corona
- Formation mechanism of corona
  - Emergence of magnetic field from disk to corona
  - Magnetic reconnection heating
- MHD simulation to Corona:
  - Magnetically supported
  - High temperature

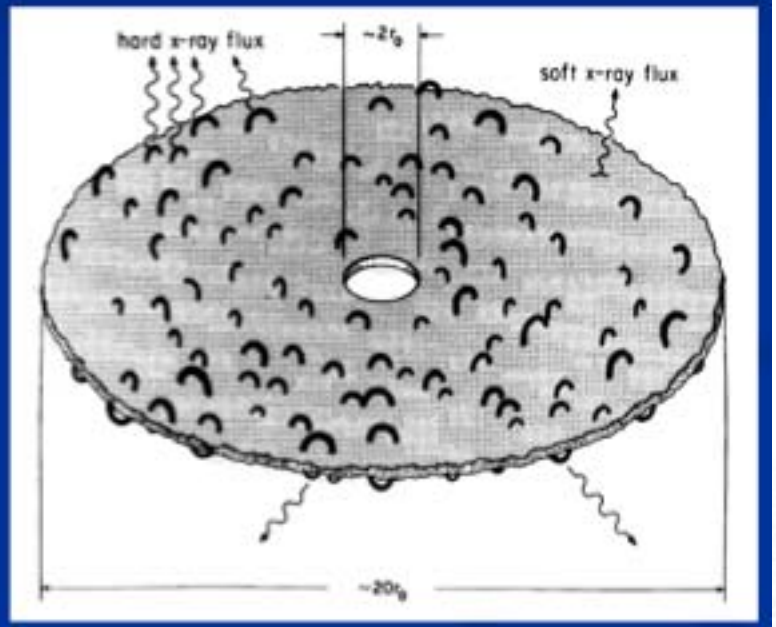

Slim and thick accretion disks

- Larger accretion rates can result in large optical depths and inefficient emission since the accretion (inflow) timescale can be shorter than the time it takes for the radiation to diffuse to the disk surface

  - photons created in radiation-pressure-dominated regions of such disks are trapped in the accretion flow and advected to the BH

  - higher T leads to slim or thick ADs

  - low radiation efficiency with $\epsilon_r < \eta$.

Photon Trapping

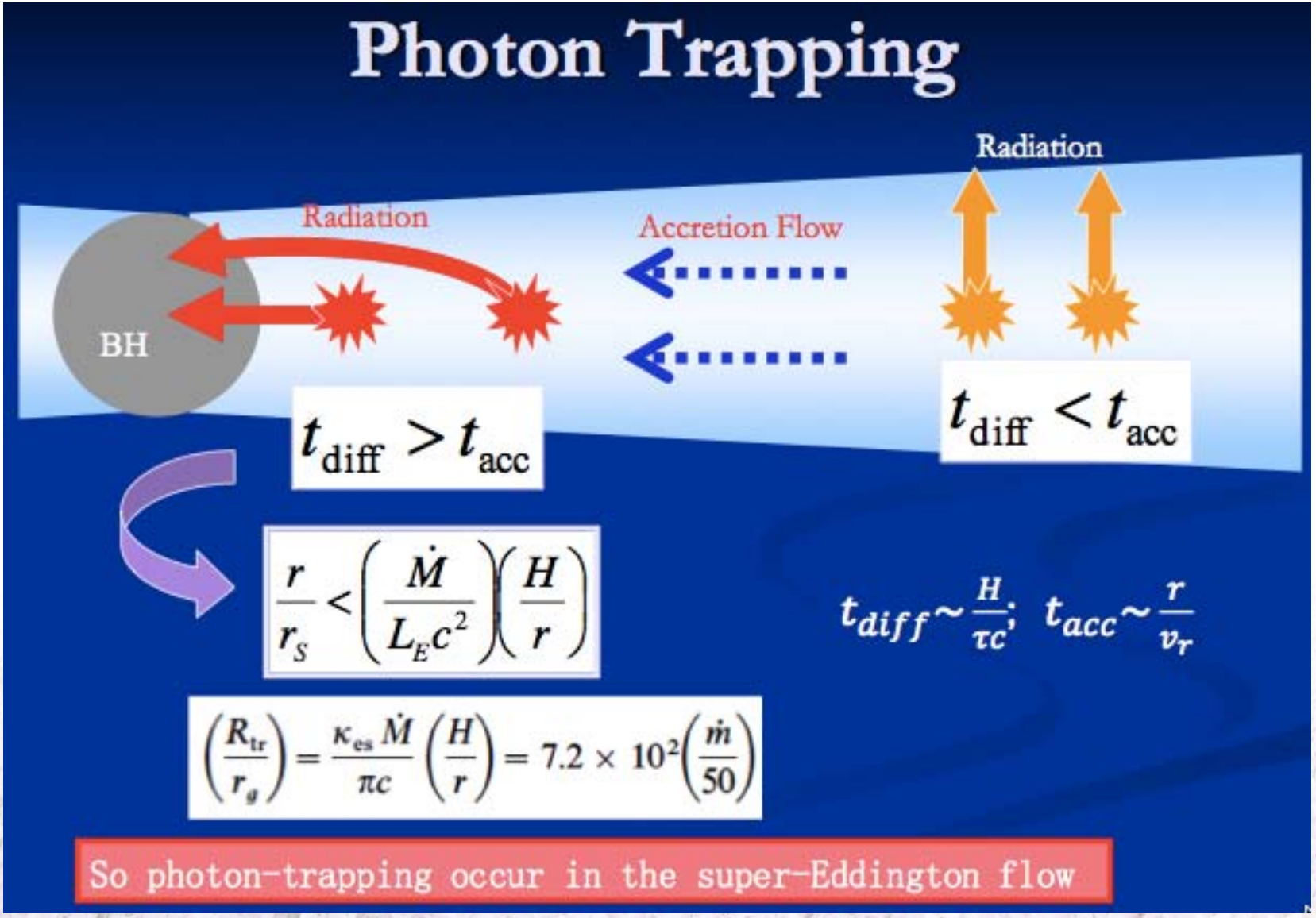

Slim disks: Radiation

- Because of advection, we have

$$T_{\rm eff}^4 \propto \frac{T_{\rm c}^4}{\tau} \propto \frac{p}{\rho H} \propto r^{-2}$$

different from the thin disk.

- Thus spectrum also changes
- Radiative efficiency lower than thin disk
- Luminosity: can be much higher than Eddington!

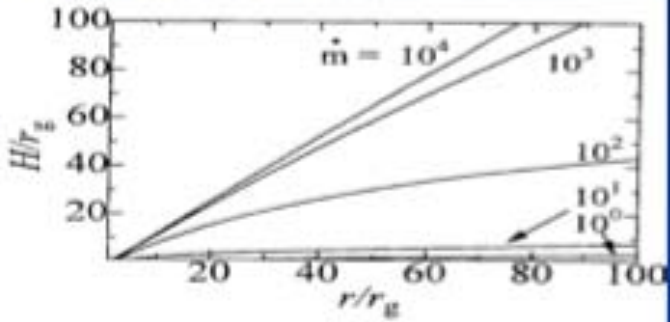

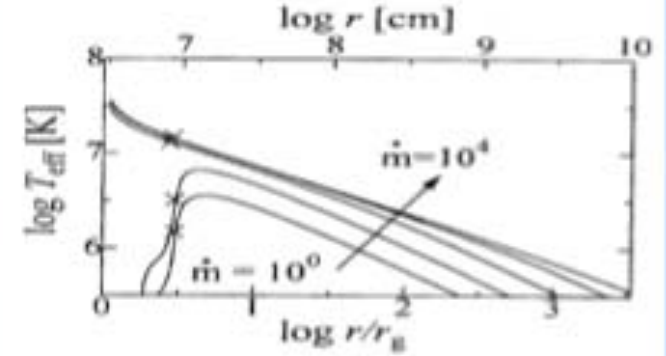

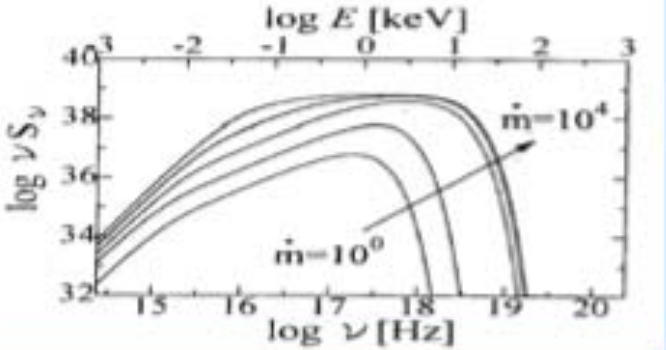

Sub-Eddington puzzle

- Slim disk: super-Eddington
- Observational results →
- Why? Feedback? unknow

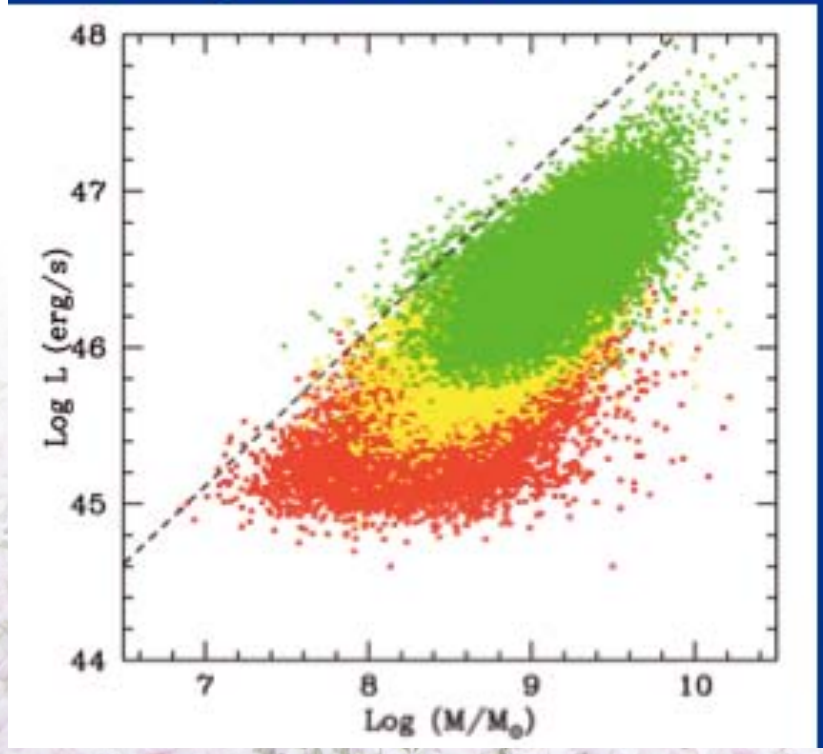

Steinhardt & Elvis 2010

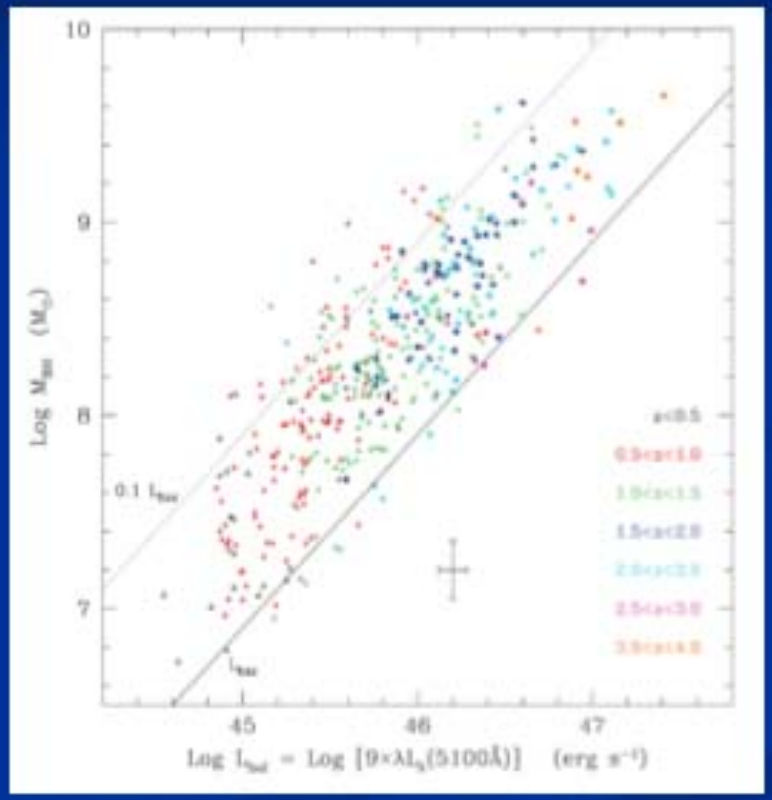

Kolleier et al. 2006

Super-Eddington Accreting Massive Black Holes as Long-Lived Cosmological Standards

Jian-Min Wang,[1,2,*] Pu Du,[1] David Valls-Gabaud,[3,1,2] Chen Hu,[1] and Hagai Netzer[4]

[1]*Key Laboratory for Particle Astrophysics, Institute of High Energy Physics, CAS, 19B Yuquan Road, Beijing 100049, China*
[2]*National Astronomical Observatories of China, CAS, 20A Datun Road, Beijing 100020, China*
[3]*LERMA, CNRS UMR 8112, Observatoire de Paris, 61 Avenue de l'Observatoire, 75014 Paris, France*
[4]*School of Physics and Astronomy and The Wise Observatory, The Raymond and Beverley Sackler Faculty of Exact Sciences, Tel-Aviv University, Tel-Aviv 69978, Israel*

(Received 27 August 2012; published 19 February 2013)

Super-Eddington accreting massive black holes (SEAMBHs) reach saturated luminosities above a certain accretion rate due to photon trapping and advection in slim accretion disks. We show that these SEAMBHs could provide a new tool for estimating cosmological distances if they are properly identified by hard x-ray observations, in particular by the slope of their 2–10 keV continuum. To verify this idea we obtained black hole mass estimates and x-ray data for a sample of 60 narrow line Seyfert 1 galaxies that we consider to be the most promising SEAMBH candidates. We demonstrate that the distances derived by the new method for the objects in the sample get closer to the standard luminosity distances as the hard x-ray continuum gets steeper. The results allow us to analyze the requirements for using the method in future samples of active black holes and to demonstrate that the expected uncertainty, given large enough samples, can make them into a useful, new cosmological ruler.

$$L_\bullet = \ell_0(1 + a \ln \dot{m}_{15})M_\bullet$$

Radiatively inefficient accretion flows

- ADs with very low accretion rates:
  - much lower densities → cooling timescale >= or >> inflow timescale
  - extremes cases of very low density:
    * cooling very inefficient
    * particles retain dissipated grav. energy for a long time
    * T rise to virial T (1e12K/r) and advected into BH without releasing E
    * called ADAFs: advection-dominated accretion flows
      - a more general term: radiatively inefficient accretion flows (RIAFs)
    * ions and electrons can have very different T (T_ion >> T_e by ~2 orders)
      - low density → less Coulomb collisions that share kinetic E
      - electrons are more efficient coolants
- Additional RIAFs: ADIOS (advection-dominated inflow outflow solution) and CDAF (convection-dominated accretion flow)

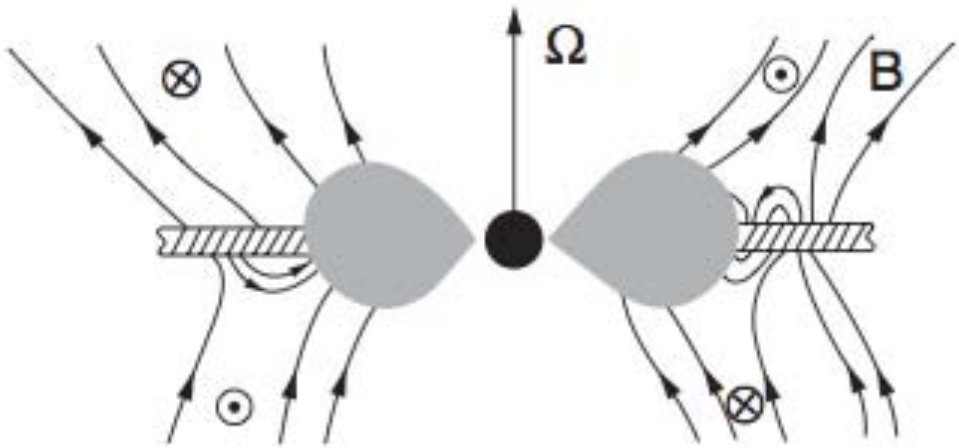

Figure 4.8. Two-temperature disks are similar to the standard optically thick, geometrically thin accretion disks far from the BH. Their very low accretion rate results in low densities and inefficient cooling in the inner parts. The gas in these regions cannot radiate away the released gravitation energy. It heats to very high temperatures, which results in a significant increase in the thickness of the disk. A large fraction of the released energy is advected to the center, and the mass-to-radiation conversion efficiency drops significantly.

Main features

- Large radial velocity:

$$v_r \sim \frac{\alpha c_s H}{R}$$

- Sub-Keplerian rotation: pressure-gradient support
- High temperature: $T \sim \frac{GMm_p}{6kR} \sim \frac{10^{12}}{r}$ (virial, why?)
- Geometrically thick: $(H = \frac{c_s}{\Omega_k} \sim R)$
- Optically thin (because of large radial velocity)
- Two-temperature: $T_i \gg T_e$
  - coupling between ions and electrons not strong enough
  - plasma collective behavior also too weak

Radiative efficiency of ADAF & LHAF

Xie & Yuan 2012

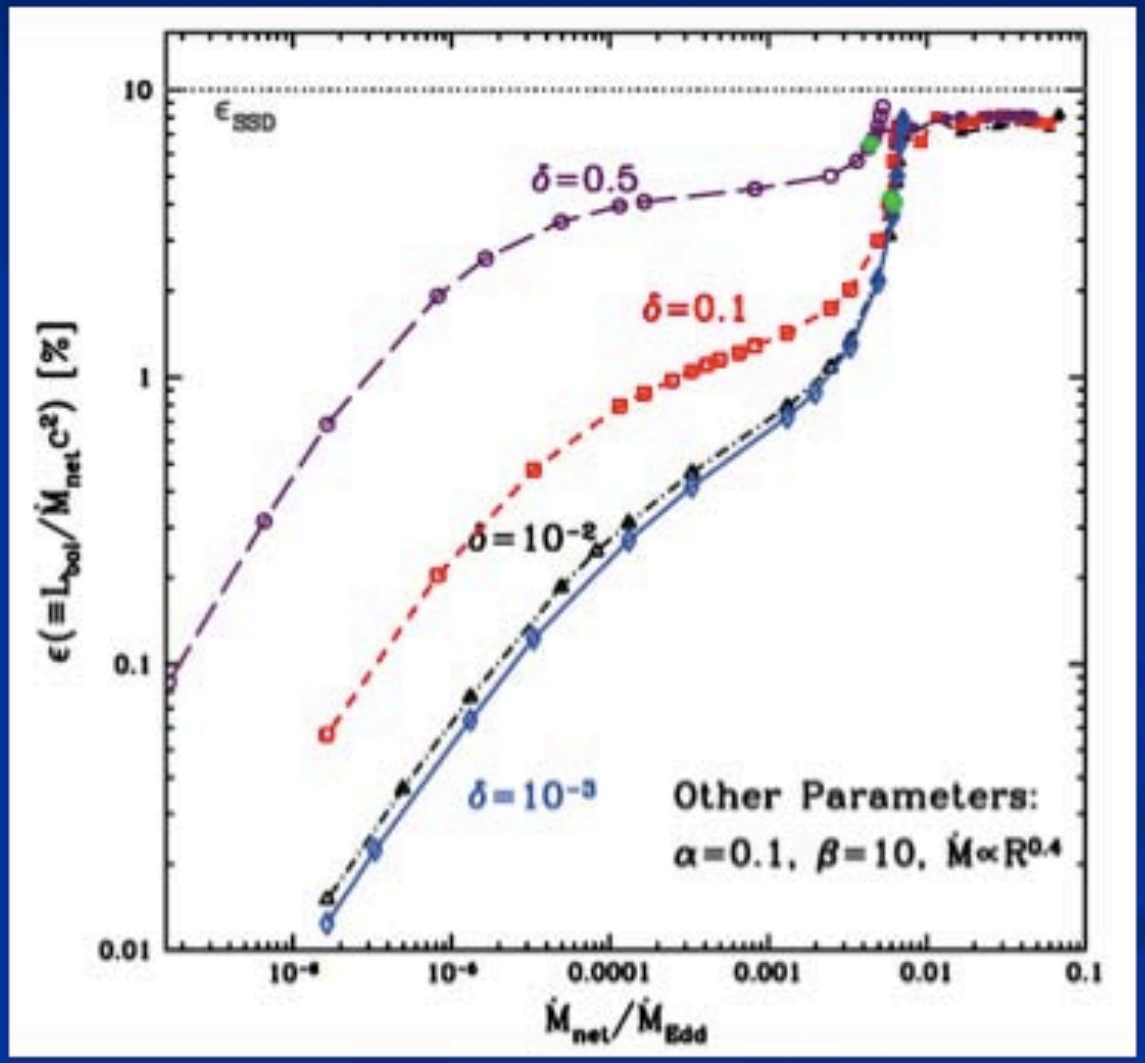

Radiative processes

- Synchrotron emission:
  - relativistic electrons & B field (described by a parameter β);
  - Maxwell distribution
  - Self-absorption of synchrotron emission
- Bremsstrahlung radiation
- Comptonization
  - seed photons are synchrotron & Brem. photons
- Misc:
  - Gamma-ray emission by the decay of neutral pions created in proton-proton collisions

Emitted Spectrum

three humps: syn. ICS Brem.

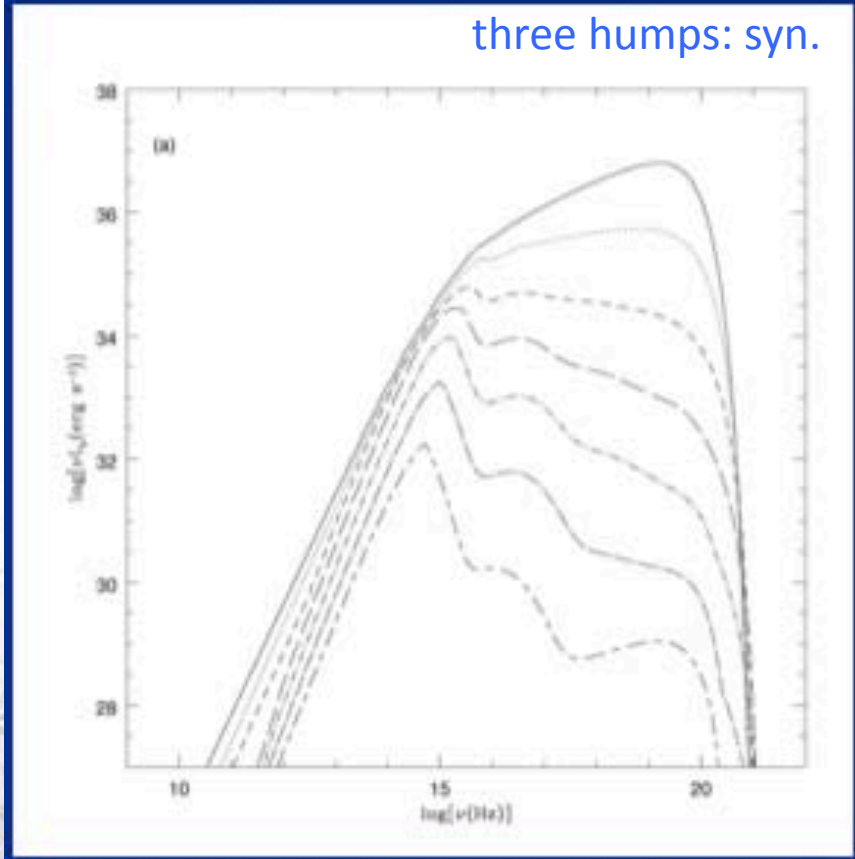

Stellar-mass BH

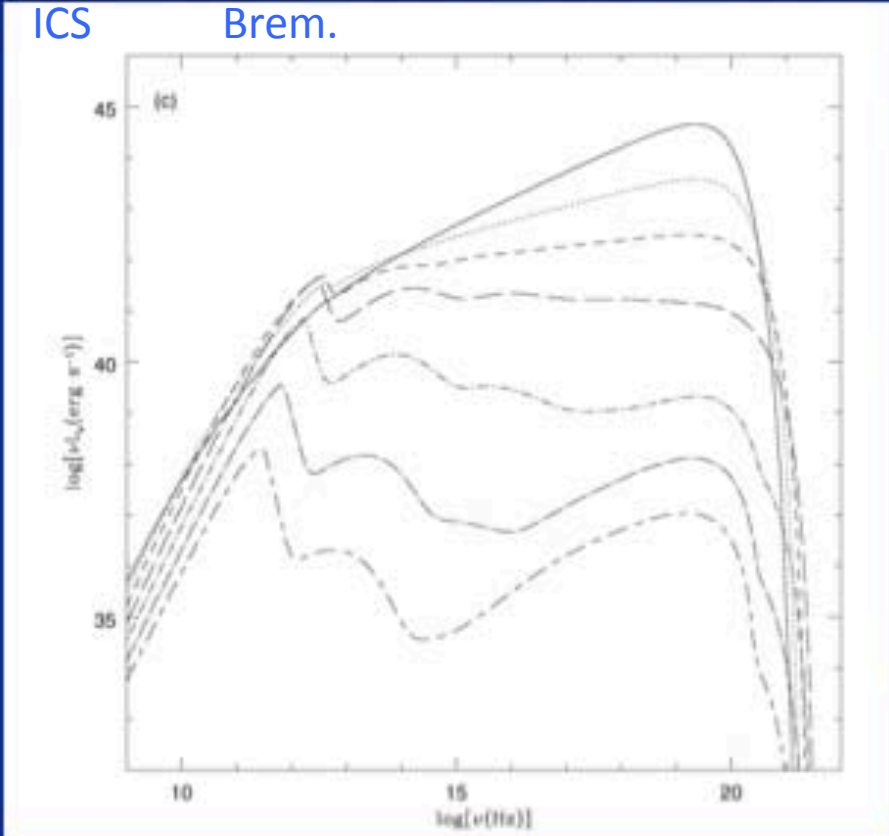

Supermassive BH

中国科学技术大学

- Various complicated numerical simulations for hot ADs being carried out:

  - GRMHD simulations: B field configuration and strength in three regions:

    * jet: - B strongest, quite ordered, large-scale poloidal B field

      - magnetic energy density > gas rest (mass) energy

    * corona: - no significant difference btw corona T and disk T (unlike SSD)

      - B strong; less ordered, turbulent, toroidal B field

      - magnetic pressure ~ gas pressure

    * main disk body: - B weak, very turbulent

      - magnetic pressure ~ 0.1*gas pressure

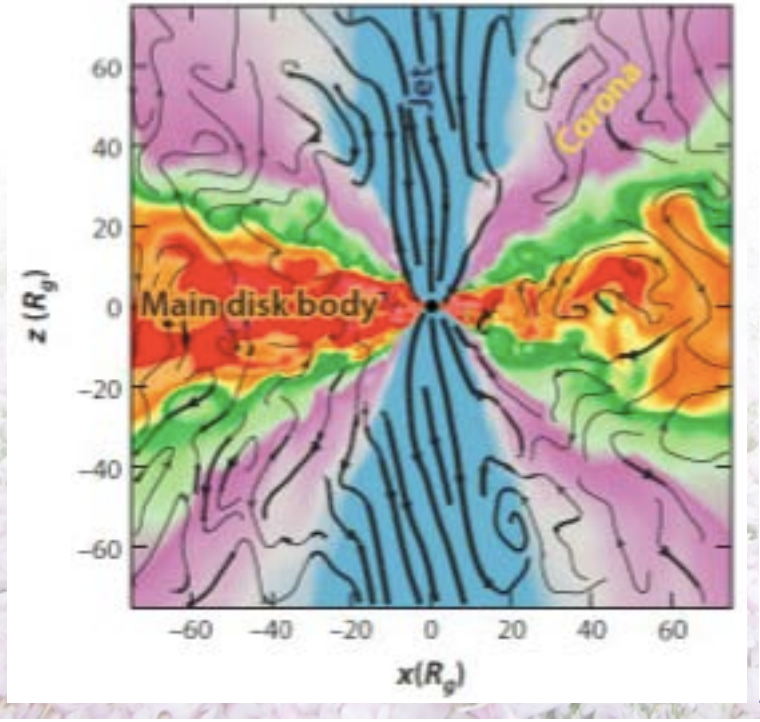

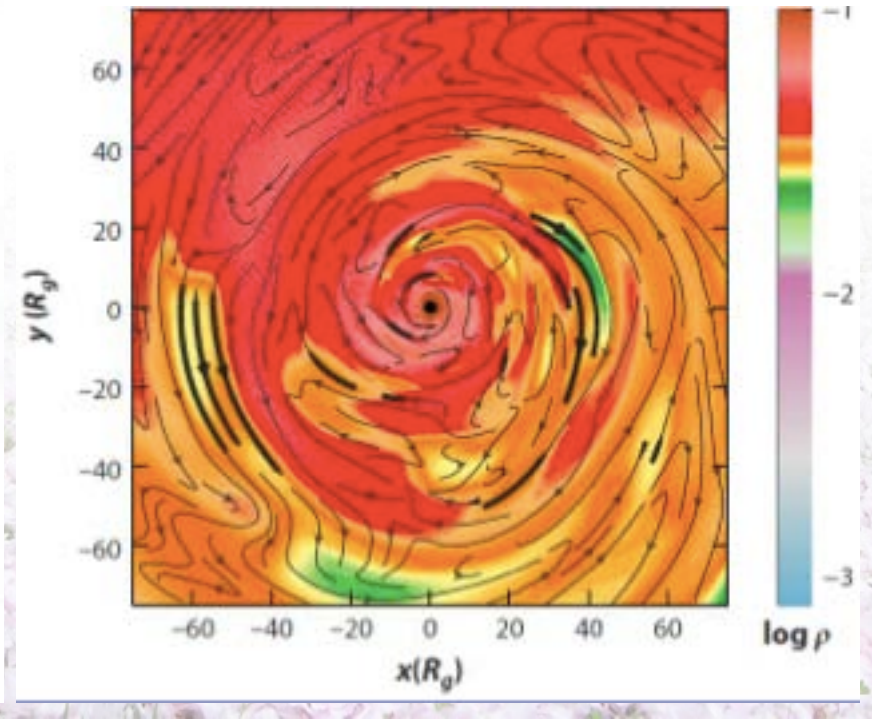

- When RIAFs involve mass loss through winds/outflows:
  - a large fraction of grav. E of inflowing gas converted to kinetic E of wind
  - such wind can leave BH on a short timescale, and move through galactic ISM or perhaps even IGM in a cluster of galaxies, delivering much of its kinetic E to the surrounding gas
    * sometimes this surrounding gas heated to emit X-ray, so can measure L_X to estimate the kinetic E of the outflow
      - some well-documented cases: $dE_K/dt > L_{bol}$
- AGN modes:
  - radiative/AGN/QSO mode: radiation-dominated processes, high L/L_{Edd}
  - radio mode: most of the released E is kinetic E, low L/L_{Edd}, observations show that such flows often associated with powerful radio jets

Mass outflows from accretion disks

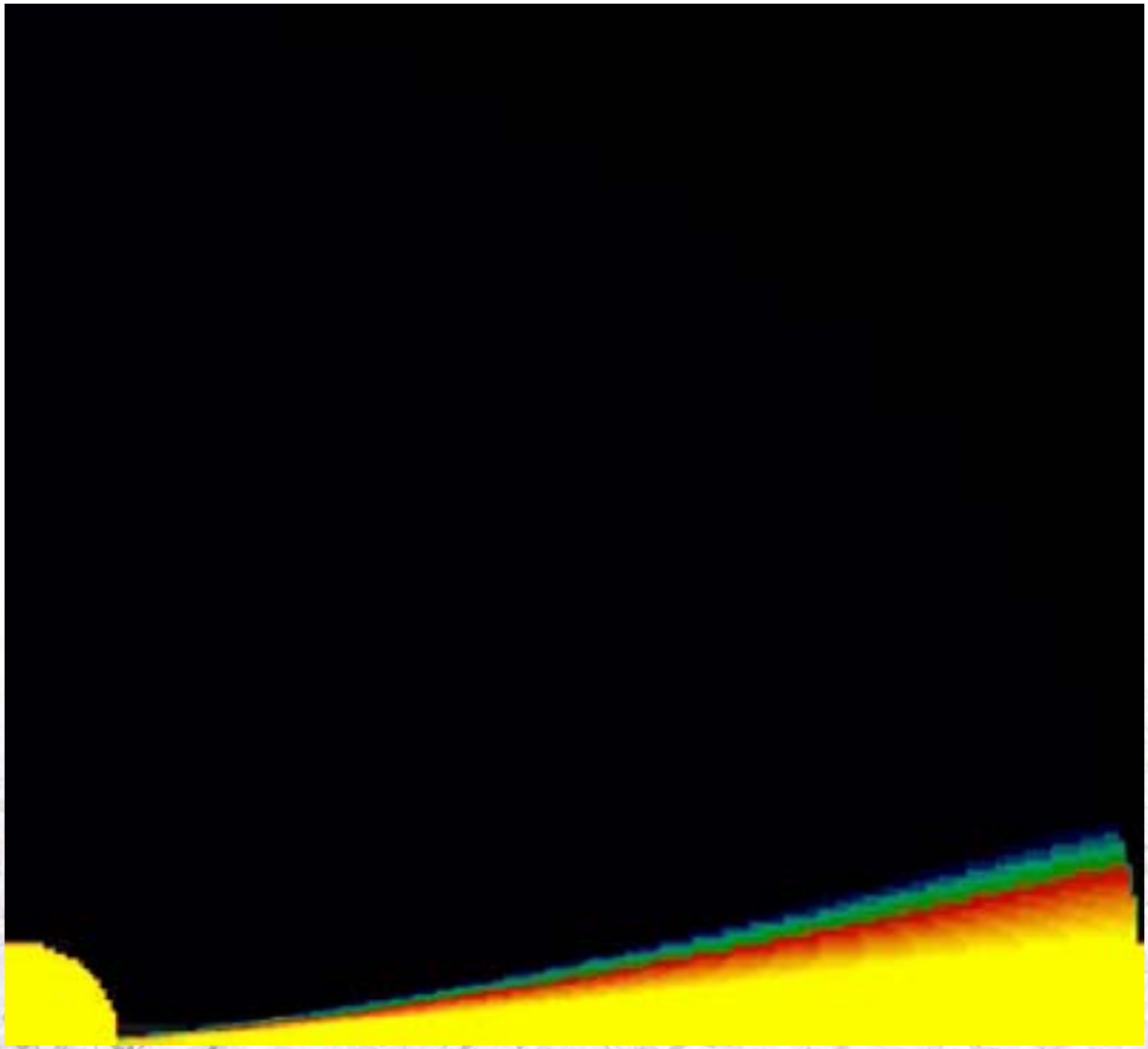

(Proga, Stone & Drew 1998, 1999)

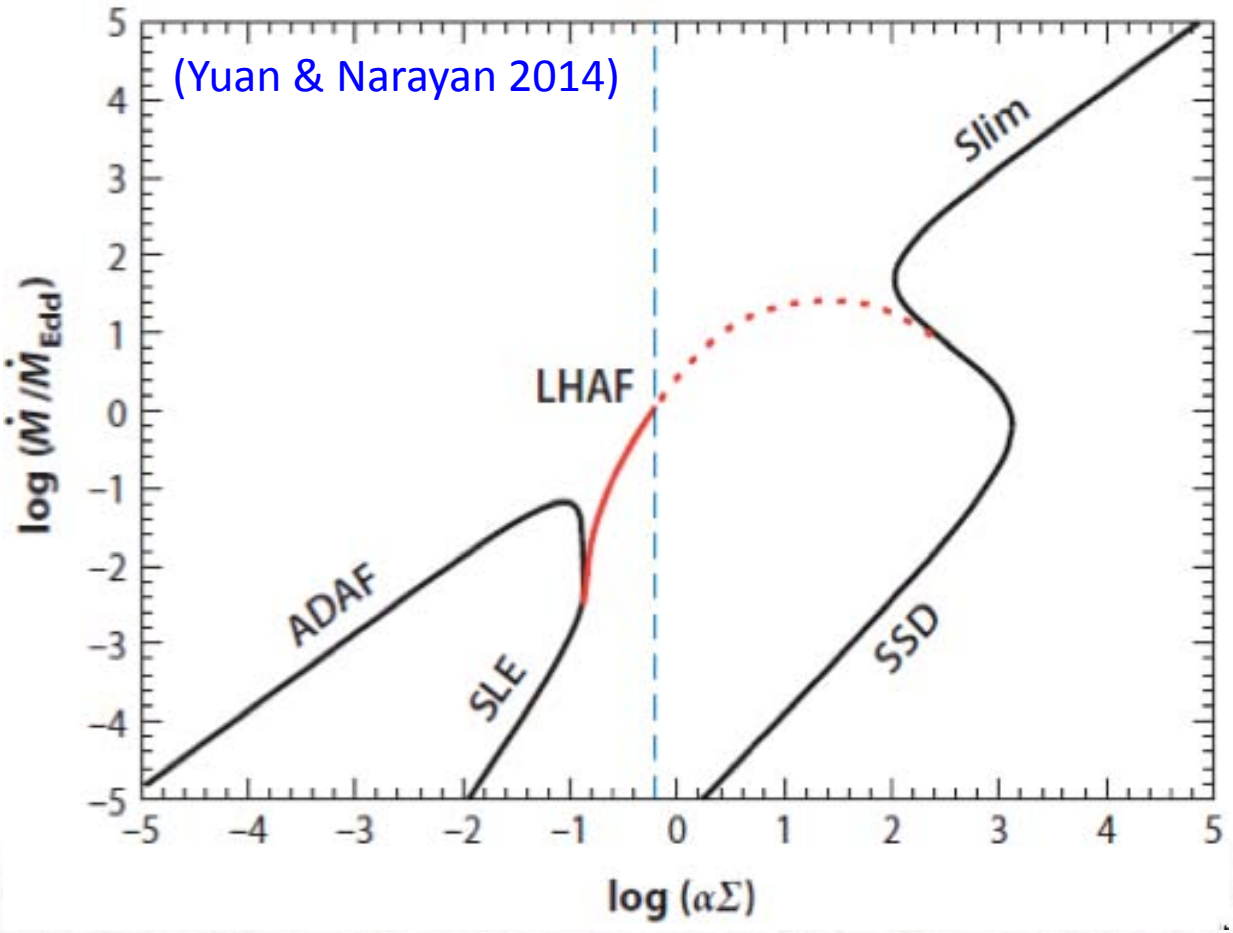

- Brief summary:
  - Accretion rate: Slim>SSD>LHAF>ADAF (holds the key)
  - Temperature: ADAF~LHAF>>Slim>SSD (hot: virial T 1e12K/r; cold: 1e6-7 K)
  - Thickness: ADAF (like spherical)~LHAF>Slim>SSD
  - Surface density: Slim>SSD>LHAF>ADAF
  - Radiation efficiency: SSD>Slim>LHAF>ADAF

Broad line region

The broad-line region

- Broad-emission-line region (BELR) or broad-line region (BLR): a typical case
  - large-column-density (~1e23 cm^{-2}), high-density (~1e10 cm^{-3}) clouds at a location of ~0.1-1 pc from BH centered at a luminous AGN with L/L_{Edd}~0.1
  - assume that clouds can survive over many dynamical times because they are confined or extensions of large self-gravitating bodies such as stars
  - clouds with large enough column densities are bound because gravity completely dominates over radiation pressure force
  - typical Keplerian velocity at this location: ~3000 km/s, reflected in line widths
  - assume a global covering factor of ~0.1-0.2, so neglect effect of radiation emitted by one cloud on its neighbors

  → the above physical properties result in $U_{hydrogen}$~0.01 and T~1e4 K

  * only illuminated surfaces of clouds are highly ionized
  * a big part of such clouds at this location must be partly neutral since only X-ray photons can penetrate beyond ~1e22 cm^{-2}
  * observed EWs of strongest lines depend on emissivity and covering factor, being of order 10-100A
  * extremely weak absorption lines expected due to small covering factor

- How many high-density clouds required to produce observed broad-line profiles?
  - given the gas velocity, and individual confined clouds likely emitting lines of ~10 km/s (the sound speed in the gas) → clouds of order of 1e6-1e8 are required to produce symmetrical smooth profiles observed in many cases
  - raise serious questions about formation and destruction of clouds and possible collisions between them
    * a possible way out: invoke internal turbulent motion exceeding sound speed by an order of magnitude or more → much broader single-cloud profiles, alleviate some of the difficulties
    * a special geometry and ordered motion of clouds can also help, e.g., a flat rotating disklike configuration
    * all these ideas need to be justified observationally and theoretically

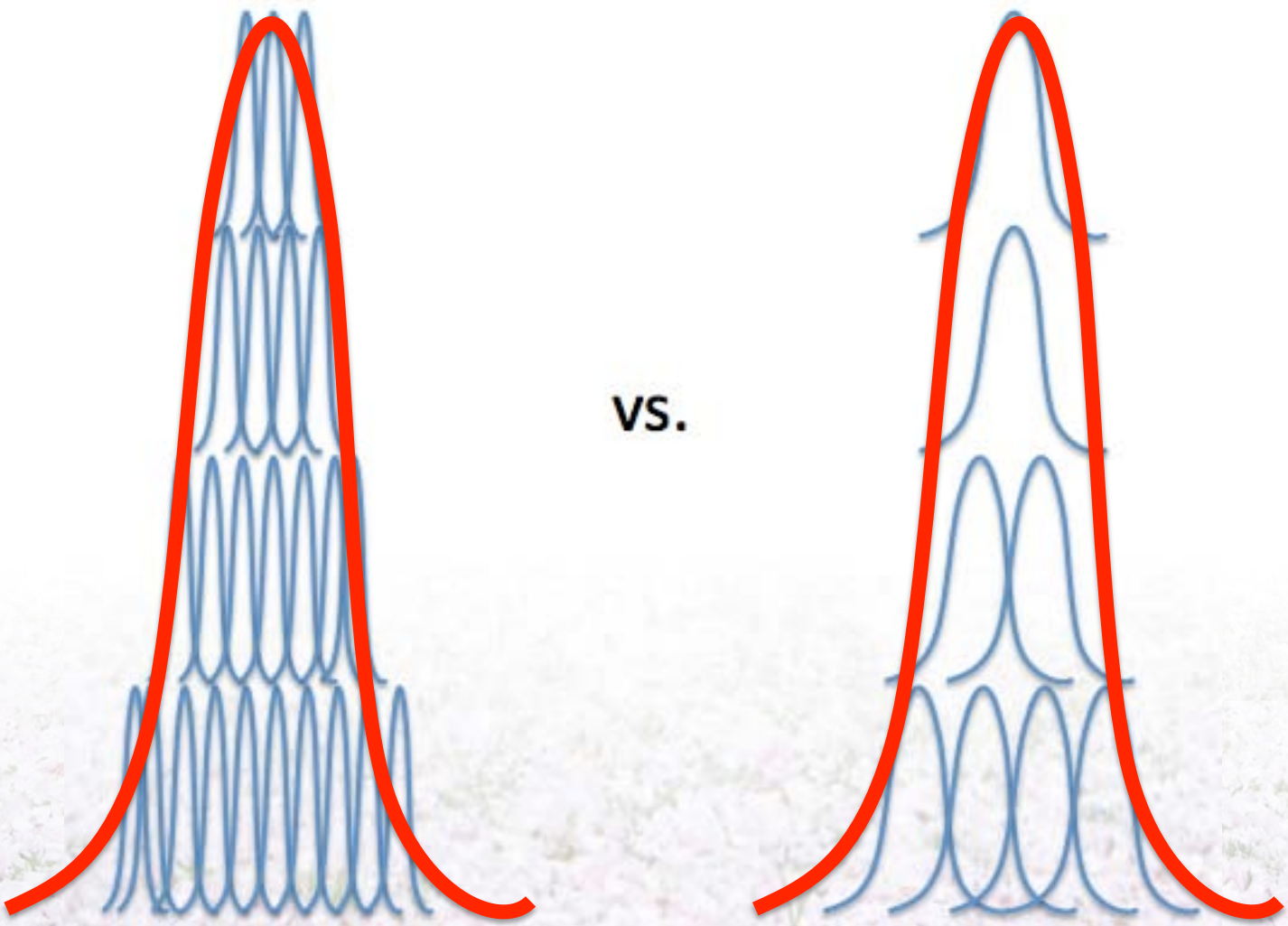

Broad-emission-line profiles

- Line profile measurements:
  - emission-line widths/profiles can differ substantially from source to source
  - but there are some general trends that are apparent in most type I sources
    * lines of more ionized species tend to be broader: consistent with a stratified, gravitationally bound BLR with higher mean ionization parameter at small distances
  - some emission lines (e.g., CIV) show lower average EWs as L increases; known as the "Baldwin effect"
  - emission-line profiles: best indicators of gas kinematics in BLR and NLR
    * numerous line and continuum processes → full, coupled solution of gas distribution, motion, and emission across BLR
    * but such solutions not available
      - line fitting by simple kinematical models gives degenerate results
      - model parameters are not linked directly to ordered motion of BLR gas
      - almost all observed profiles are consistent with randomly oriented orbits in a gravitationally bound cloud system

- A small number of well-observed sources: unique double-peak line profiles
  - most are Halpha, sometimes Hbeta, and few MgII lines
  - most are radio-loud AGNs seen at a relatively large inclination angle
  - fraction of broad, double-peak emission-line AGNs is very small (much below 10%); but similar, more smooth profiles can be due to some emissivity patterns across a flat inclined disk – such sources can be more numerous
  - currently no complete models to explain all line intensities, profiles, variability

(double-peaked Halpha lines; Eracleous & Halpern 2003)

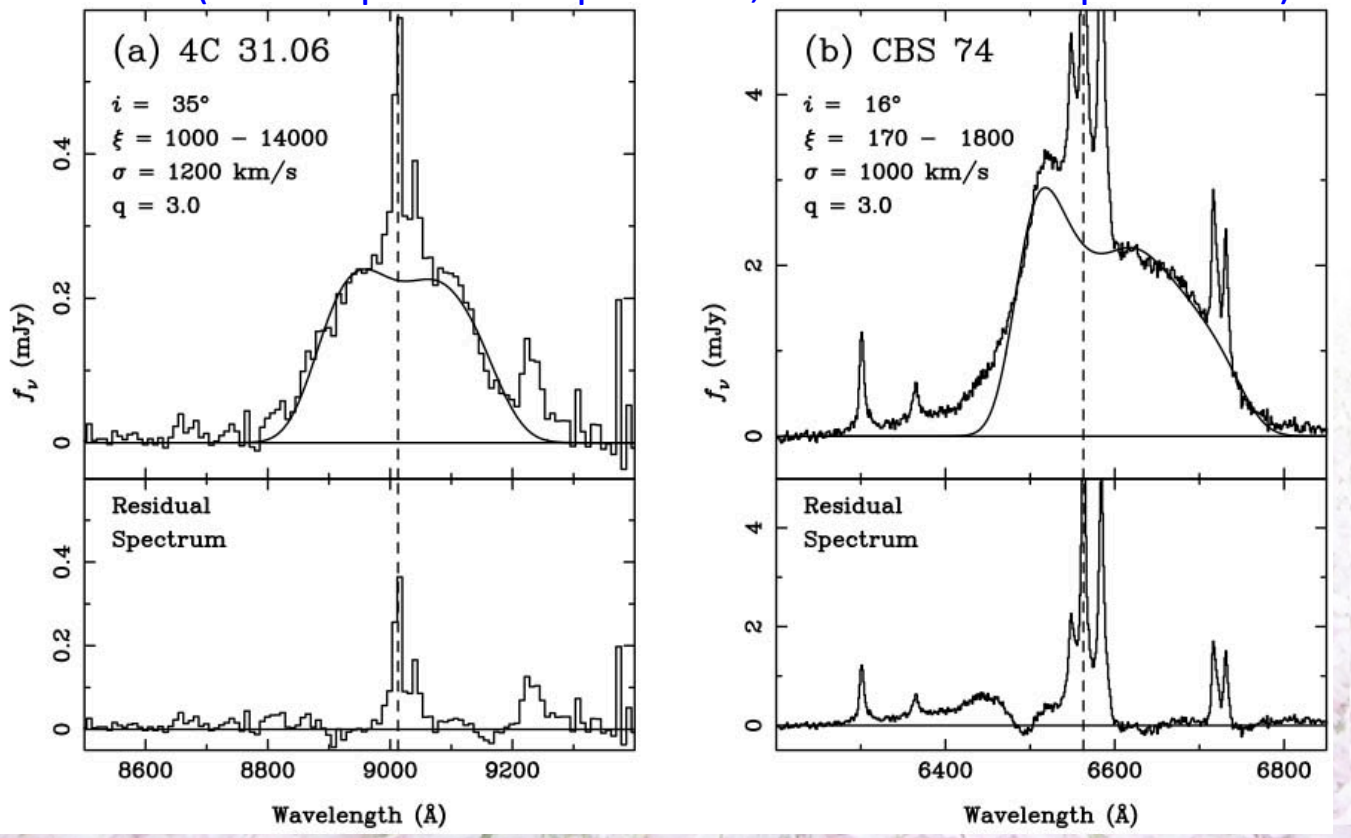

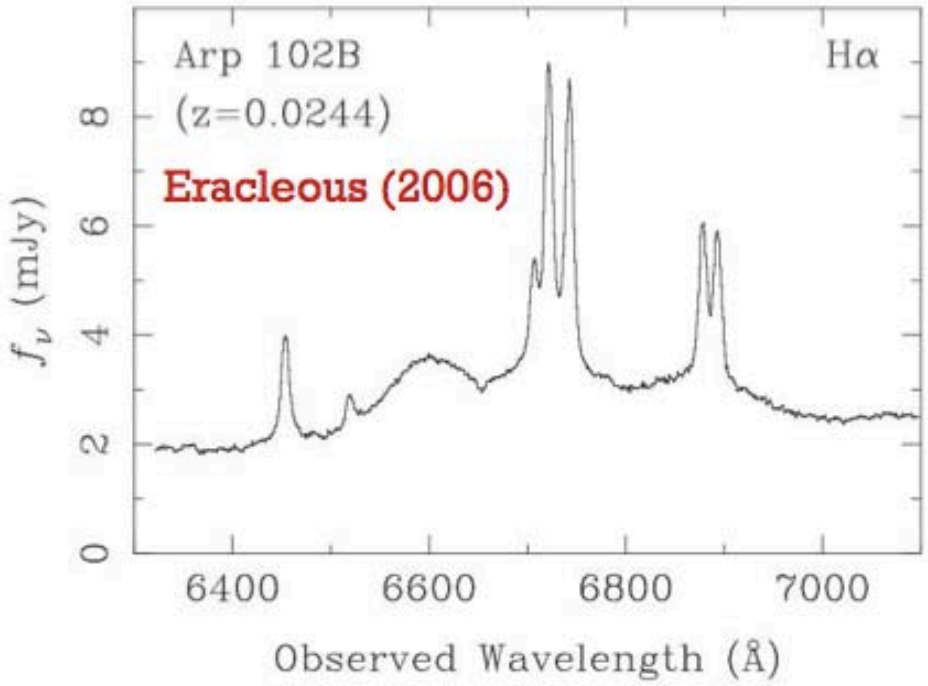

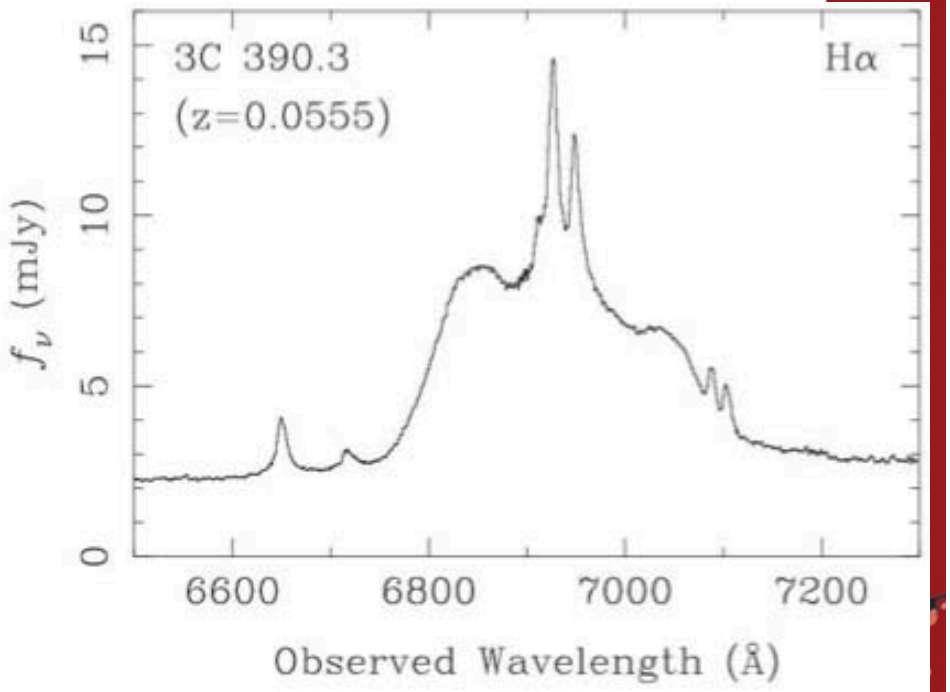

Figure 2. The observed Hα spectra of Arp 102B and 3C 390.3 as examples of double-peaked Balmer emission lines. The approximate full widths of the lines at half maximum are 16,000 km s^{-1} and 12,000 km s^{-1}, respectively.

Characteristic of rotating disks – some of the BLR emission from a disk?

Double-peaked BLR lines can show complex variability patterns.

Eigenvector 1

- Several well-established correlations in type I AGNs appear under the name "eigenvector 1": first found by PCA of low-z AGN spectra
  - first principal component (PC1/eigenvector 1): has the largest possible variance (i.e., accounts for as much of the variability in the data as possible)
  - e.g., the largest amount of variance (eigenvector 1) is caused by strengths of the FeII and [OIII] lines which are strongly anticorrelated

(Boroson & Green 1992)

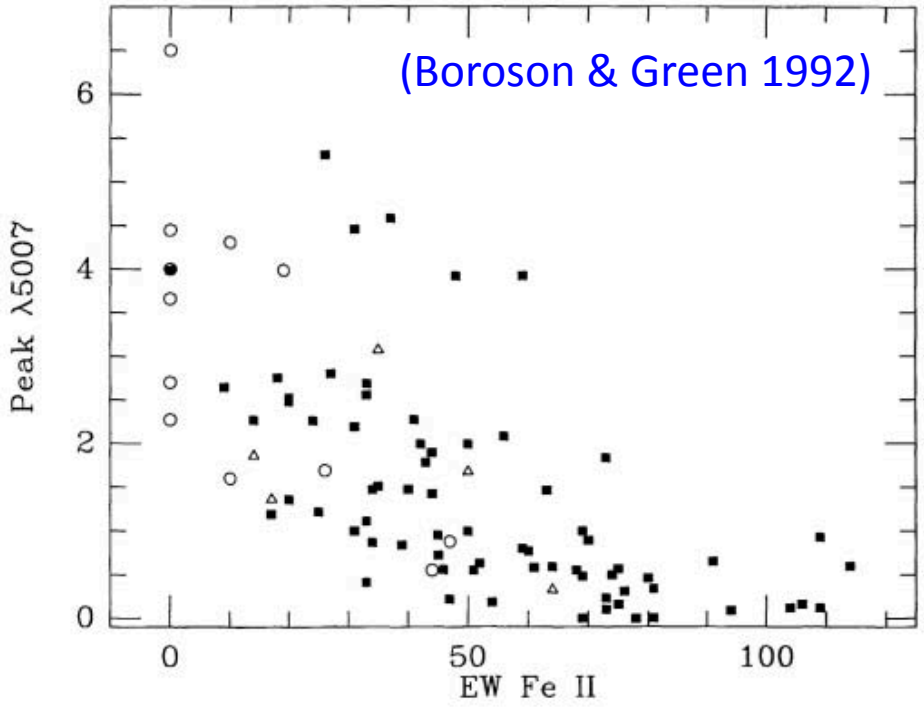

FIG. 2.—Ratio of peak height of [O III] λ5007 to that of Hβ plotted against equivalent width of the Fe II emission between λ4434 and λ4684. Solid squares are radio-quiet objects, open circles are steep-spectrum radio sources, and open triangles are flat-spectrum radio sources.

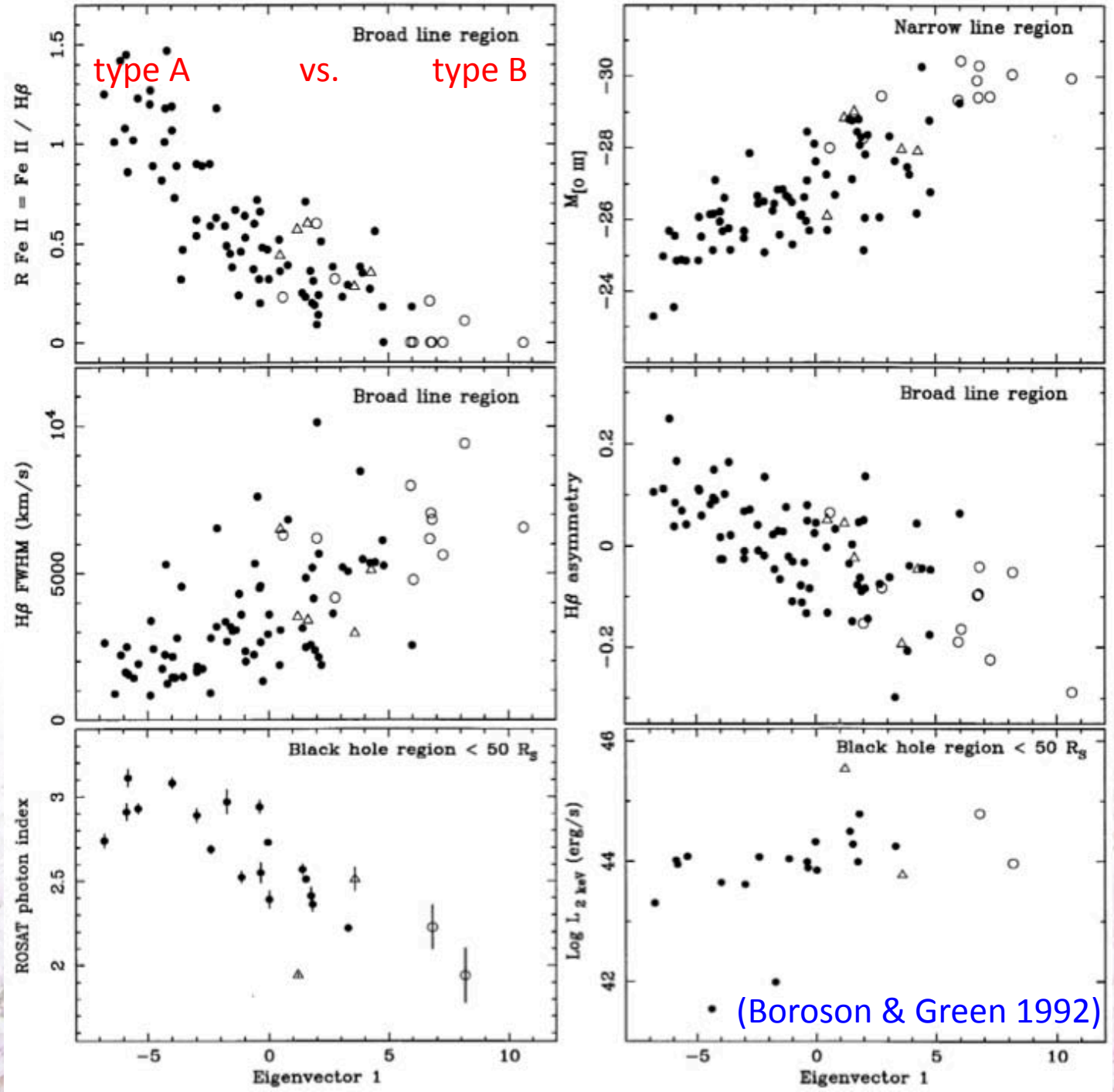

(Boroson & Green 1992)

The diversity of quasars unified by accretion and orientation

Yue Shen & Luis C. Ho

Affiliations | **Contributions** | **Corresponding author**

Nature **513**, 210–213 (11 September 2014) | doi:10.1038/nature13712

Received 30 March 2014 | Accepted 23 July 2014 | Published online 10 September 2014

Quasars are rapidly accreting supermassive black holes at the centres of massive galaxies. They display a broad range of properties across all wavelengths, reflecting the diversity in the physical conditions of the regions close to the central engine. These properties, however, are not random, but form well-defined trends. The dominant trend is known as 'Eigenvector 1', in which many properties correlate with the strength of optical iron and [O III] emission[1, 2, 3]. The main physical driver of Eigenvector 1 has long been suspected[4] to be the quasar luminosity normalized by the mass of the hole (the 'Eddington ratio'), which is an important parameter of the black hole accretion process. But a definitive proof has been missing. Here we report an analysis of archival data that reveals that the Eddington ratio indeed drives Eigenvector 1. We also find that orientation plays a significant role in determining the observed kinematics of the gas in the broad-line region, implying a flattened, disk-like geometry for the fast-moving clouds close to the black hole. Our results show that most of the diversity of quasar phenomenology can be unified using two simple quantities: Eddington ratio and orientation.

Emission-line variability and reverberation mapping

- Optical-UV continuum L and broad emission-line variations in all type I AGNs:
  - can be observed given long enough time
  - strongly correlated line and continuum variations
    * line L change follows continuum L change: strongest, clearest evidence that src. of ionization and heating of BLR gas is the central ionizing continuum
    * time lag btw continuum and line variation → simple estimate of BLR size (light travel time), which is L dependent and ~5-500 light days

  [narrow lines do not vary on short timescales, indicating they are from a much larger region]
- reverberation mapping (RM): several big campaigns follow such variations over months and years to obtain info of gas & ionization distribution, gas kinematics
  - idea: time-delayed, Doppler-shifted response of a system to a known input signal can be used to infer structure and kinematics of the responding system
  - by means of transfer function: describe the response of the line light curve upon the continuum light curve

Broad Lines Lag Continuum

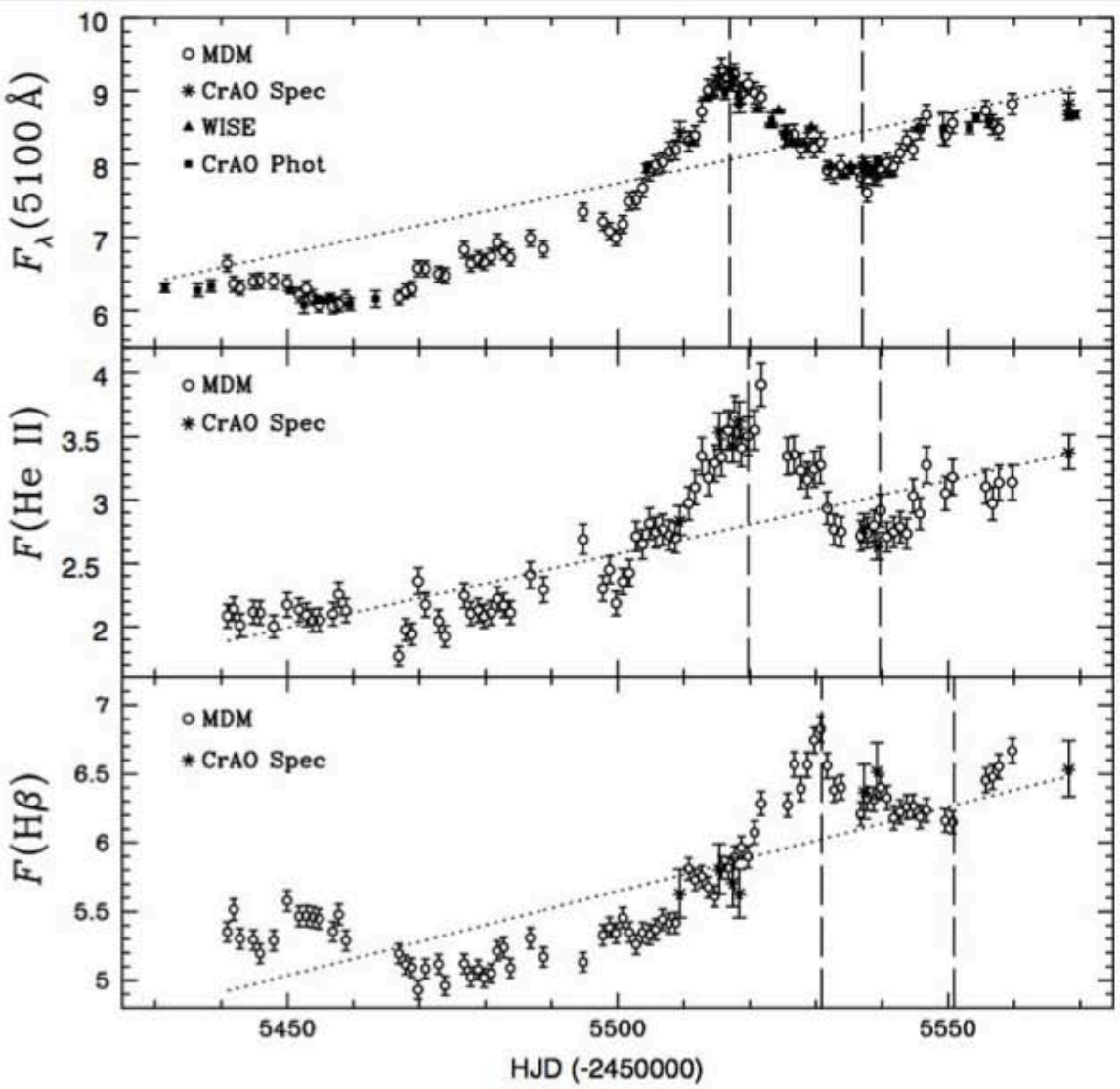

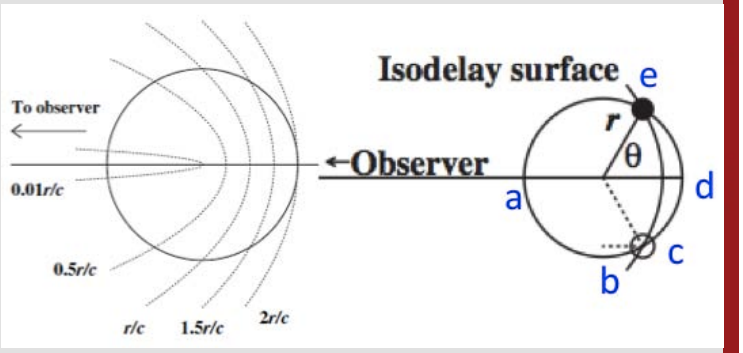

Figure 2. Complete light curves for Mrk 335 from our observing campaign. The top panel shows the 5100 Å flux in units of 10^{-15} erg s^{-1} cm^{-2} Å^{-1}, the middle panel shows the flux in the He II λ4686 region in units of 10^{-13} erg s^{-1} cm^{-2}, and the bottom panel shows the integrated Hβλ4861 flux, also in units of 10^{-13} erg s^{-1} cm^{-2}. Open circles denote observations from MDM Observatory and asterisks represent spectra taken at CrAO. Closed squares show the photometric observations from CrAO, and closed triangles represent photometric observations from WISE Observatory. Vertical dashed lines have been placed at two obvious features in the continuum to aid the eye. The vertical lines have been shifted by the measured He II and Hβ lag values (2.7 days and 13.9 days, respectively) to aid the eye in identifying the correct lag values for each emission line. Dotted lines show the trends that were subtracted before performing the cross-correlation analysis.

Grier et al. (2012)

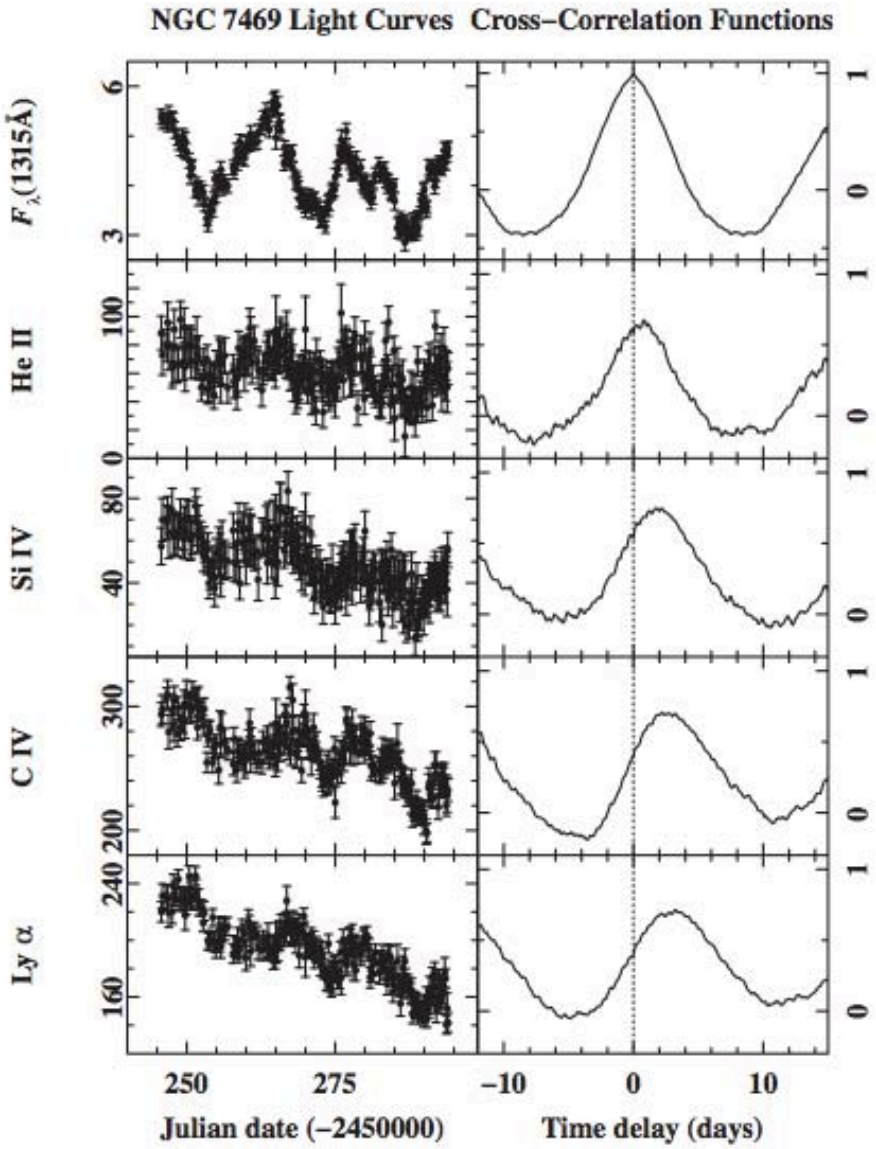

Figure 7.10. (left) The light curves of NGC 7469 obtained with IUE during an intensive AGN Watch monitoring campaign during summer 1996. (right) CCFs obtained by cross-correlating the light curve immediately to the left with the 1315 Å light curve at the top of the left column. The panel at the top of the right column thus shows the 1315 Å continuum autocorrelation function (ACF).

Size of the Broad Line Region

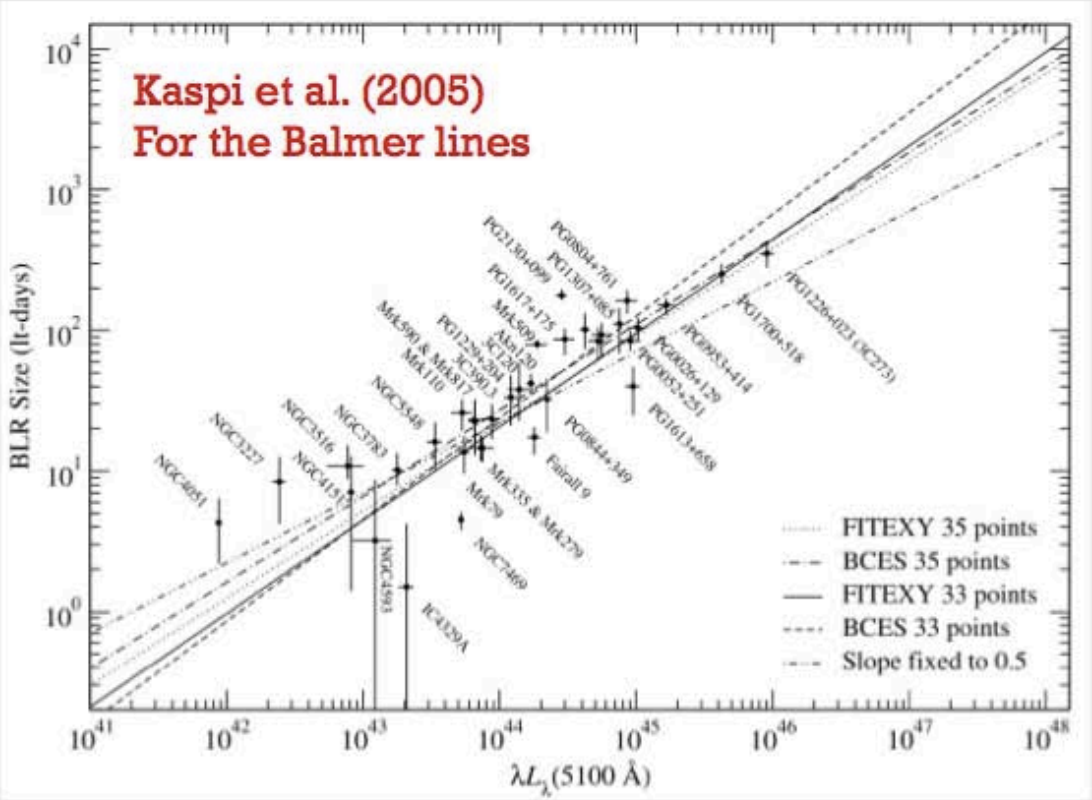

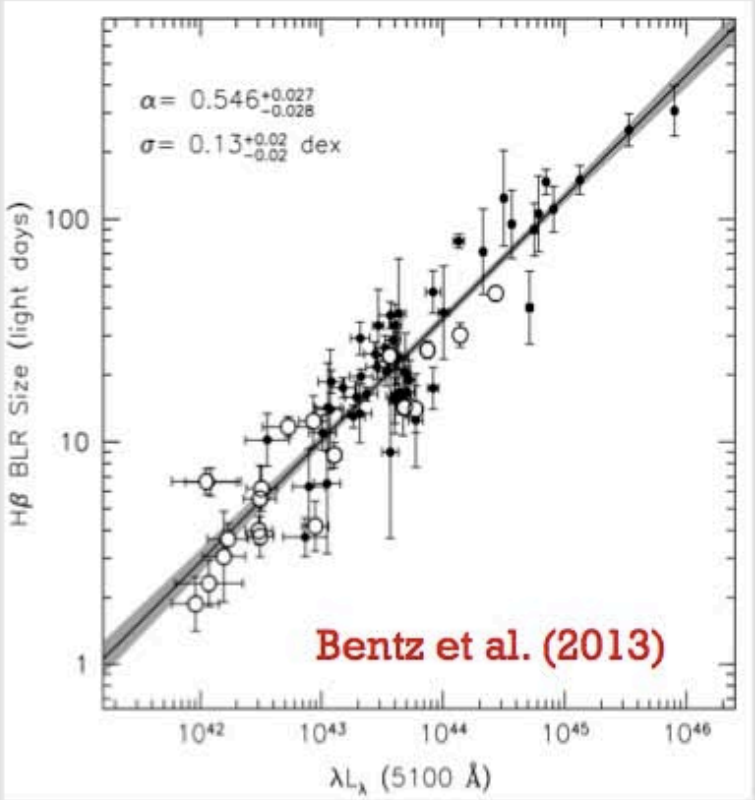

The BLR radius is found to scale as $R_{BLR} \sim L^{0.5\text{-}0.7}$.

The slope is about as expected if all AGNs have similar ionization parameters and densities in their BLRs ($r \sim L^{0.5}$).

Reverberation Mapping: Stratification and Virialization

Reverberation lags have now been measured for ~ 50 AGNs.

The current sample is biased toward AGNs with relatively strong lines.

Mostly measured for Hβ, but in some cases for multiple lines.

The highest ionization emission lines respond most rapidly to continuum changes, indicating ionization stratification.

A plot of line width vs. lag (τ) shows that $v \sim \tau^{-0.5}$, as expected for virialized gas dominated by the gravitational potential of the central source.

But must still worry about other effects, especially radiation pressure.

Evidence for Virialization

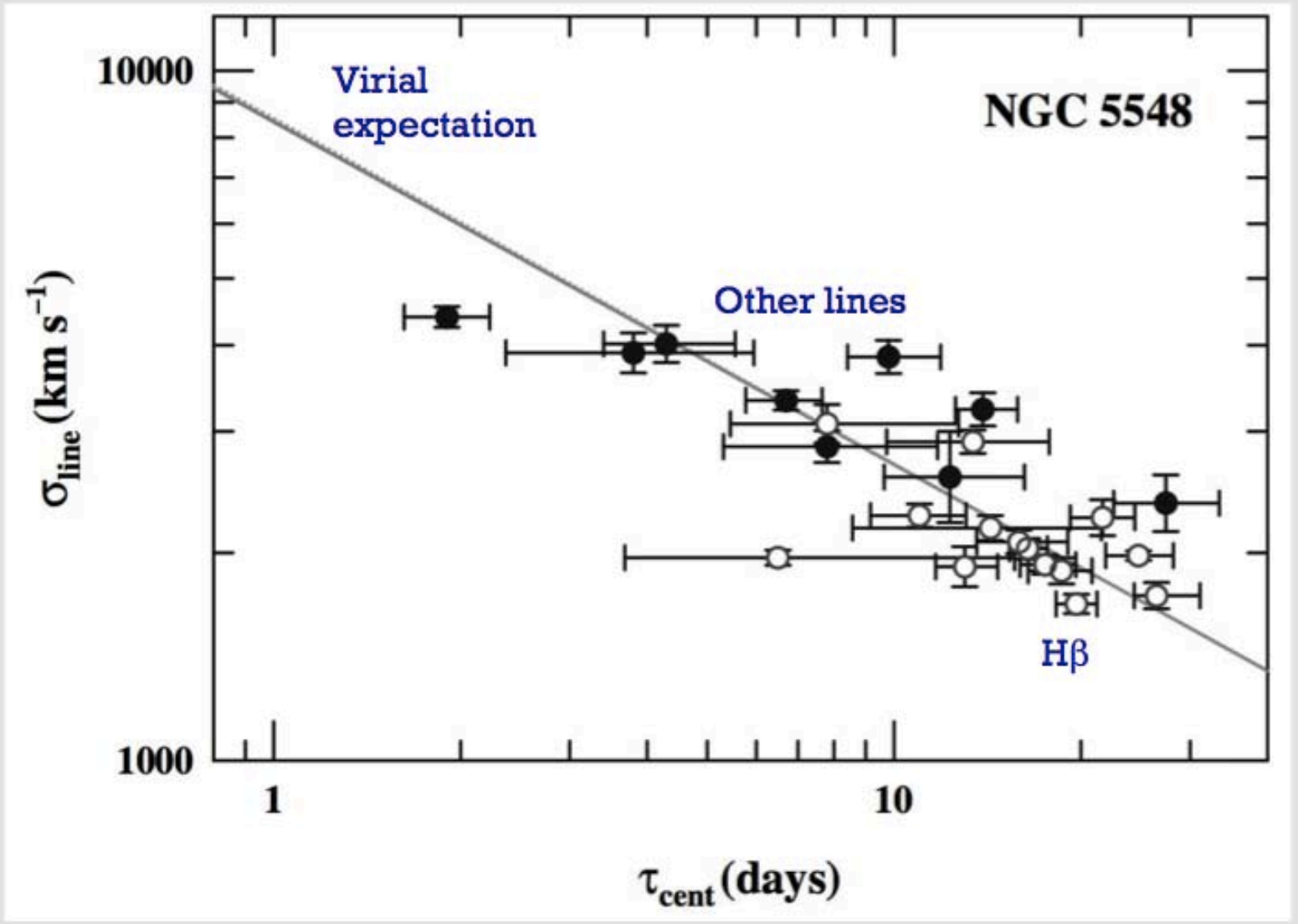

Peterson et al. (2004)

BLR "Breathing"

In a few well-studied objects the BLR has been observed to "breathe" over ~ year timescales, appearing to become larger as a source varies to high luminosities.

The BLR gas itself does not expand and contract under such "breathing". It is moving much too slowly for this.

Rather, there is gas everywhere in the line-emitting region, and what changes with luminosity is the distance from the continuum source where conditions are optimal for line emission.

This idea is called the "local optimally emitting cloud" (LOC) model.

Total reservoir of gas present is ~ 1000-10000 $M_{\odot}$, though only a small fraction of this (less than ~ 1%) radiates lines efficiently at a given time.

Example of BLR "Breathing"

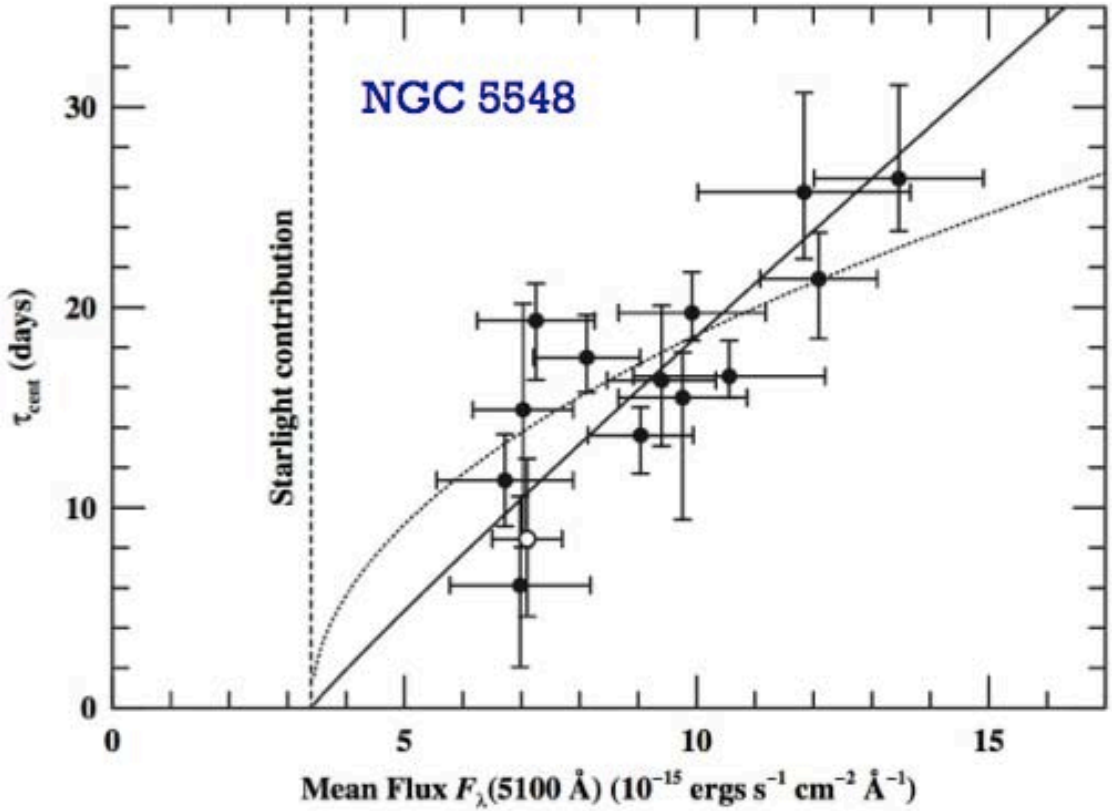

Fig. 7. Measured time delays for Hβ in NGC 5548 versus optical continuum flux for 14 independent experiments. The vertical line shows the constant stellar contribution to the measured continuum flux. The best-fit slope to this relationship is shown as a solid line $\tau(\mathrm{H}\beta) \propto F_\lambda^{0.9}$ and the dotted line shows the naive prediction $\tau(\mathrm{H}\beta) \propto F_\lambda^{1/2}$. From [27]

Peterson et al. (2002)

- common assumption: the system is virialized and individual clouds are moving in their own Keplerian orbits not necessarily with the same inclination and eccentricity

Estimating Black Hole Masses

Can estimate black-hole masses following the virial theorem:

$$M_{\rm BH} = \frac{f c\tau \Delta V^2}{G}$$

Where *f* is a factor that includes (unknown) BLR geometry and inclination.

Comparison with other mass-estimation methods indicates an average value of $f \sim 4$-5.

Masses measured this way appear accurate to within a factor of ~ 3 when Hβ is used.

Note this method can be used, if patient, for masses at high redshifts.

Mass-Luminosity Relationship

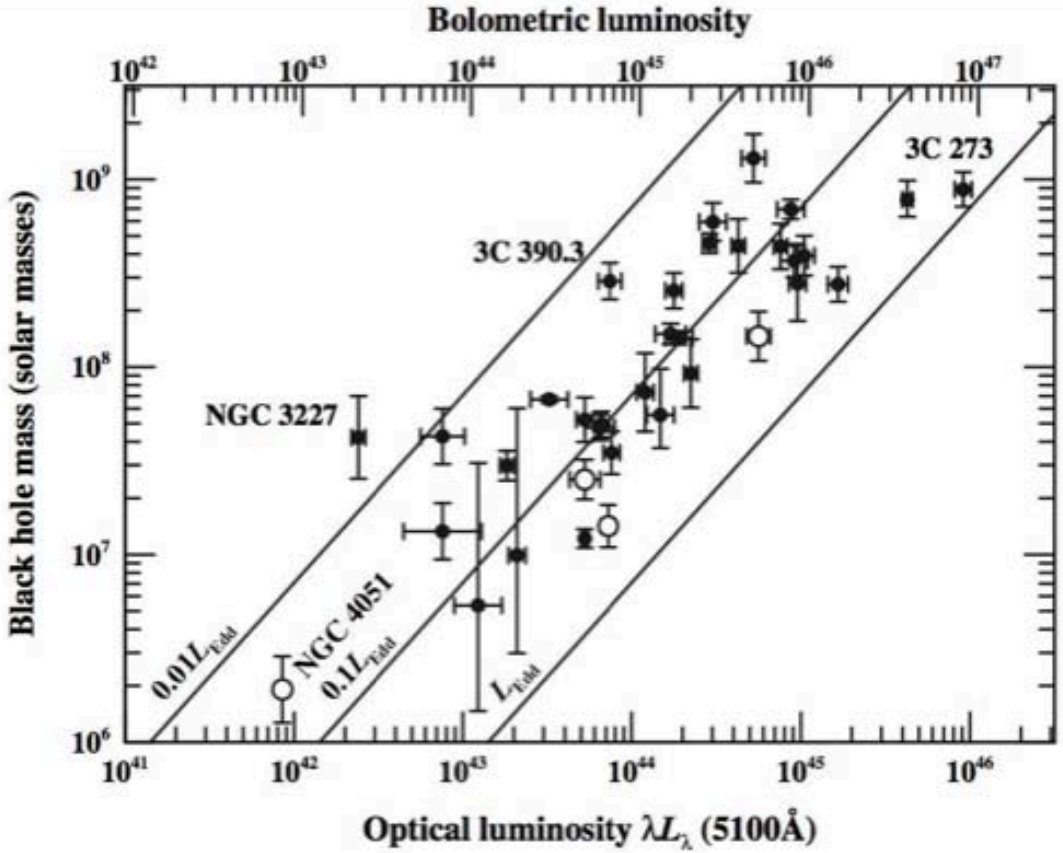

Fig. 9. The mass–luminosity relationship for reverberation-mapped AGNs. The luminosity scale on the lower x-axis is $\log \lambda L_\lambda$ in units of ergs s^{-1}. The upper x-axis shows the bolometric luminosity assuming that $L_{\rm bol} \approx 9\lambda L_\lambda(5100\,\text{Å})$. The *diagonal lines* show the Eddington limit $L_{\rm Edd}$, $0.1L_{\rm Edd}$, and $0.01L_{\rm Edd}$. The *open circles* represent NLS1s. From [25]

Peterson et al. (2004)

Single-Epoch Masses

Can combine the R_{BLR}-L relation with the virial theorem to estimate single-epoch masses. For example…

$$\frac{M_{BH}}{10^6\ M_\odot} = 4.35 \left[\frac{\nu L_\nu(5100\ \text{Å})}{10^{44}\ \text{ergs s}^{-1}}\right]^{0.7} \left[\frac{\text{FWHM(H}\beta)}{10^3\ \text{km s}^{-1}}\right]^2$$

Similar relations exist for Mg II and C IV.

These allow quick estimates for large AGN samples, but their accuracy is no better than a factor of several. The main challenge is characterizing the line widths, where caution is needed.

Statistical use of such masses in large samples is probably OK, but individual mass estimates may be unreliable.

What is the Nature of the BLR?

After much research, it is appearing increasingly likely that the BLR itself has a composite nature:

Moderate-ionization and high-optical-depth region

- Largely responsible for the Balmer-line emission and Mg II
- Accretion disk itself?
- A disk with a large line-emitting region can make single-peaked profiles consistent with most objects

High-ionization and moderate-optical-depth region

- Largely responsible for the high-ionization lines
- Accretion-disk wind?
- Helps explain blueshifts of high-ionization lines and blueward line asymmetries

The end